

**Synthesis And Characterization Of Cobalt/Iron Nanocatalyst Via
Reverse Microemulsion Method**

by

Muhammad Nur Azizi bin Abdul Aziz

10853

Dissertation submitted in partial fulfillment of
the requirements for the
Bachelor of Engineering (Hons)
(Chemical Engineering)

SEPTEMBER 2011

University Teknologi PETRONAS
Bandar Seri Iskandar
31750 Tronoh
Perak Darul Ridzuan

CERTIFICATION OF ORIGINALITY

This is to certify that I am responsible for the work submitted in this project, that the original work is my own except as specified in the reference and acknowledgements, and that the original work contained herein have not been undertaken or done by unspecified sources or person.



.....
(MUHAMMAD NUR AZIZI BIN ABDUL AZIZ)

TABLE OF CONTENT	PAGE
CHAPTER 1 INTRODUCTION	1
1.1 BACKGROUND STUDY.....	1
1.2 PROBLEM STATEMENT.....	2
1.3 OBJECTIVE AND SCOPE OF STUDY.....	3
1.4 RELEVANCY OF THE PROJECT.....	4
1.5 FEASIBILITY OF THE PROJECT.....	4
CHAPTER 2 LITERATURE REVIEW	5
2.1 INTRODUCTION TO FISCHER-TROPSCH TECHNOLOGY....	5
2.2 FT PRODUCT DISTRIBUTION.....	6
2.3 CATALYSTS FOR FT SYNTHESIS.....	7
2.4 CARBON NANOTUBE SUPPORTER.....	9
2.5 MICROEMULSION METHOD.....	11
2.5.1 Introduction.....	11
2.5.2 Preparation of Nanoparticles.....	12
2.5.3 Influence of Various Factors on the Particle.....	15
2.5.3.1 <i>Size of the Water Droplets</i>	15
2.5.3.2 <i>Surfactant Concentration</i>	16
2.5.3.3 <i>Nature of the Reducing Agent</i>	16
2.5.4 Advantages and Disadvantages of Microemulsion Method	16
2.6 CRITICAL MICELLE CONCENTRATION.....	17
2.7 CATALYST ANALYSIS.....	19
2.7.1 Transmission Electron Microscopy Analysis (TEM).....	20
2.7.2 Field Emission Scanning Electron Microscopy Analysis (FESEM).....	21
2.7.3 Energy Dispersive X-ray Analysis (EDX).....	21
2.7.4 Surface Area Analysis (BET).....	21
CHAPTER 3 METHODOLOGY	23
3.1 CALCULATION.....	23
3.1.1 Dilution of Nitric Acid for Purification of CNT.....	23
3.1.2 Amount of Iron and Cobalt Nitrate for Catalyst Preparation.....	23

3.1.3 Molarity of Triton X-114 in Cyclohexane.....	24
3.1.4 Ratio of Water-Surfactant.....	24
3.1.5 Amount of Hydrazine.....	25
3.2 PREPARATION OF Co/Fe CATALYSTS.....	25
3.3 PROJECT ACTIVITIES.....	26
3.4 KEY MILESTONE/GANTT CHART.....	28
3.5 TOOLS/EQUIPMENTS/CHEMICAL REQUIRED.....	29
CHAPTER 4 RESULT AND DISCUSSION.....	27
4.1 DATA GATHERING AND ANALYSIS.....	30
4.1.1 Determination of Water-To-Surfactant Ratio.....	30
4.2 ANALYSIS ON CHARACTERIZATION METHODS.....	32
4.2.1 Particle Size Distribution.....	32
4.2.2 Surface Morphology and Element Composition.....	40
4.2.3 Energy Dispersive X-ray Spectroscopy (EDX) Analysis.....	42
4.2.4 Texture Properties of Nanocatalyst.....	42
4.2.5 Fischer-Tropsch Performance.....	43
CHAPTER 5 CONCLUSION AND RECOMMENDATION.....	46
REFERENCES.....	48
APPENDICES.....	51

LIST OF TABLES	PAGE
<i>2.1 Metal Cost for FT.....</i>	8
<i>2.2 Comparison between Cobalt and Iron Catalysts.....</i>	9
<i>3.1 Appropriate Amount of Metals.....</i>	24
<i>3.2 Volume of Water for Applied Amount of Surfactant.....</i>	24
<i>3.3 Amount of Hydrazine versus Fe/Co.....</i>	25
<i>3.4 Composition of Fe VS Co.....</i>	26
<i>3.5 Weekly Work Progression.....</i>	27
<i>3.6 Important Date.....</i>	29
<i>3.7 Proposed Gantt Chart.....</i>	29
<i>3.8 Tools/Equipment/Chemicals for FYP.....</i>	29
<i>4.1 Average Particle distribution for inner and outer surface of CNT..</i>	39
<i>4.2 Overall average particle size and standard deviation.....</i>	39
<i>4.3 Weight percentage of element on nanocatalyst.....</i>	42
<i>4.4 Properties of the catalysts.....</i>	43

LIST OF FIGURES	PAGE
2.1 <i>Carbon Nanotubes</i>	10
2.2 <i>The microscopic structure of a microemulsion at a given concentration of surfactant as function of temperature and water concentration</i>	11
2.3 <i>Modes of particle preparation from microemulsion: (a) Mixing of two microemulsion; (b) Direct addition of reducing agent to the microemulsion</i>	13
2.4 <i>Principal Stages in the Preparation of Fe/Vo Supported FT Catalyst</i>	14
2.5 <i>Principal stages of metal nanoparticle preparation using microemulsion</i>	14
2.6 <i>Amphiphilic Molecules</i>	18
2.7 <i>Critical Micelle Concentration</i>	19
4.1 <i>Water to surfactant (6 : 1)</i>	30
4.2 <i>Water to surfactant (7 : 1)</i>	31
4.3 <i>Water to surfactant (8 : 1)</i>	31
4.4 <i>TEM images of 100Co/CNT at different magnification</i>	33
4.5 <i>TEM images of 90Co10Fe/CNT at different magnification</i>	34
4.6 <i>TEM images of 80Co20Fe/CNT particle at different magnification</i>	35
4.7 <i>TEM images of 70Co30Fe/CNT particle at different magnification</i>	36
4.8 <i>Metal distribution of pure cobalt catalyst</i>	37
4.9 <i>Metal distribution of 90Co10Fe/CNT</i>	37
4.10 <i>Metal distribution of 80Co20Fe/CNT</i>	38
4.11 <i>Metal distribution of 70Co30Fe/CNT</i>	38
4.12 <i>FESEM images of 100Co/CNTBI</i>	41
4.13 <i>FESEM images of 90Co10Fe/CNT</i>	41
4.14 <i>FESEM images of 80Co20Fe/CNT</i>	41
4.15 <i>FESEM images of 70Co30Fe/CNT</i>	41

<i>4.16 Percentage of CO conversion at different composition.....</i>	41
<i>4.17 Percentage of product selectivity at different composition.....</i>	42

LIST OF APPENDICES	PAGE
<i>Appendix 3.1 Calculation of HNO₃ dilution.....</i>	52
<i>Appendix 3.2 Calculation of metal precursor.....</i>	52
<i>Appendix 3.3 Calculation of surfactant and cyclohexane.....</i>	54
<i>Appendix 4.1 Spectrum processing from FESEM.....</i>	55
<i>Appendix 4.2 Electron images from EDX.....</i>	57
<i>Appendix 4.3 Calculation of average particle size and population standard deviation.....</i>	61

CHAPTER 1

INTRODUCTION

1.1 BACKGROUND STUDY

Sabatier and Senderens have been known as the pioneers of catalytic hydrogenation of carbon monoxide which established the first experiment in 1902. During the period, methane was produced from a mixture of CO and CO₂ gases under 1 atm pressure at 453 – 473K. It was then continued by Hans Fischer and Franz Tropsch under Synthol process which operated the experiment above 100 bar. The process managed to produce a mixture of aliphatic oxygenated compounds through the reaction of CO₂ with H₂ at 673K. A mixture of hydrocarbon called Synthine was produced when the product was heated under pressure. In 1923, it was reported that more heavy hydrocarbons could be produced at lower pressure which below than 7 bar.

Since the discovery of Fischer Tropsch (FT) reaction in 1920s, metals of cobalt (Co) and iron (Fe) have been chosen to be the industrial catalysts due to its ability to boost the reaction. The metals are used in combination with various ranges of supports and promoters that permits further control over the products selectivity. In particular, it has been reported that combination of Co and Fe at certain composition has generated more products rich in olefins and alcohols rather than the usage of single metal alone (Tavasoli et al., 2009; Duvenhage & Coville, 1997).

One of the methods of preparing the catalyst is the reverse microemulsion method. This method enables the control of metal particle size with a narrow size distribution, despite of metal content. The size of particles formed in water-in-oil microemulsion can be

controlled by changing the micelle size (water-to-surfactant ratio). It has been reported that the catalyst prepared by water-in-oil microemulsion increases the CO hydrogenation and H₂ chemisorption rate as well as C₂ + selectivity. In addition, this method has increased the activity of Fe/SiO₂ catalyst as compared to the same average particle size catalyst prepared by incipient wetness impregnation method (Trépanier et al., 2010).

1.2 PROBLEM STATEMENT

The declining of worldwide reserve crude oil has been a controversial issue. This major problem has led to the incremental price of worldwide fuel oil and it is forecasted to be continuously increasing from time to time. While the nation is settling the problem of fuel oil issue, there is one unique process existed since the early of 20th century which is proved can convert synthesis gas mainly hydrogen and carbon monoxide as the key ingredients to precious line of hydrocarbon products. The process is well known as Fischer-Tropsch process where it is said to produce liquid hydrocarbon products from natural gas. Apparently, catalyst is very important in order to gain better performance and at the same time it reduces the selectivity of methane which is an unwanted product. As the catalyst is made, it is important to ensure that the preparation method of the catalyst is done accordingly to result in better catalyst's activity and selectivity.

The reverse microemulsion method has been proposed to produce the catalyst. Base on earlier works, this method is better as compared to other existed method such as precipitation method and impregnation method due to its uniqueness. However, the current experimental practices only focus on the production of a catalyst containing monometallic either Co or Fe. In Final Year Project, student will be introduced to the bimetallic via certain compositions to produce a better catalyst. Through the best bimetallic composition, the activity and selectivity of the catalyst can be enhanced.

1.3 OBJECTIVE AND SCOPE OF STUDY

The objectives of the project are:

- To prepare a bimetallic catalyst consists of Co and Fe in different composition on CNT support via reverse microemulsion method.
- To characterize the bimetallic catalyst in term of composition, morphology and texture properties.
- To study the properties of the catalyst by applying several characterization methods which are Transmission Electron Microscopy (TEM), Field Emission Scanning Electron Microscopy (FESEM), Energy Dispersive X-ray Spectroscopy (EDX) and surface area analysis (BET).
- To study the performance of Fischer-Tropsch reaction.

The scope of study of the project is:

- Setting up a laboratory scale experiment for Fischer-Tropsch process to study the effect of Fe/Co catalyst prepared by reverse microemulsion method.
- Studying the effects of different ratio of iron and cobalt which differs the properties of the catalysts.
- Studying the characterization methods which are Transmission Electron Microscopy (TEM), Field Emission Scanning Electron Microscopy (FESEM), Energy Dispersive X-ray Spectroscopy (EDX) and surface area analysis (BET).
- Determining the composition of Fe/Co on the catalyst which gives the best performance base on the activity and selectivity of the catalyst.

1.4 RELEVANCY OF THE PROJECT

This project is a relevant project since it may give a positive result of the performance of FT catalyst throughout the experimental practices by applying different method other than the existed such as impregnation and precipitation method. Moreover, the reverse microemulsion method is so far one of the methods which gives a good result on the activity and selectivity of the catalyst. Thus, to obtain a more promising result, a single metal of Fe is combined with Co to form bimetallic to test whether the outcome catalyst would improve instead of using only one single metal.

1.5 FEASIBILITY OF THE PROJECT

The reverse microemulsion method is suitable to be done in laboratory as there are accommodation, tools, equipment and also chemicals which are the main elements to determine whether this project may excel or not. The time given to conduct the experiment is also sufficient and reasonable which consists of the period of preparing the catalyst until testing the catalyst in the microreactor.

CHAPTER 2

LITERATURE REVIEW

2.1 INTRODUCTION TO FISCHER-TROPSCH TECHNOLOGY

Fischer-Tropsch (FT) technology can be briefly defined as the process used to convert synthesis gas containing hydrogen (H_2) and carbon monoxide (CO) to produce hydrocarbon products. The hydrocarbon products are mostly liquid at ambient conditions but some are formed in gaseous and some may be even in solid form. The hydrocarbon products include the formation of oxygenated hydrocarbons such as alcohols excluding methanol (Steynberg, 2004, p. 1-63).

Nowadays, interest in FT technology is increasing rapidly. This is due to recent improvement to the technology which it can be used to obtain value from natural gas reserve. In other words, the natural gas reserve will be converted to liquid hydrocarbon product that can be sold in the worldwide market.

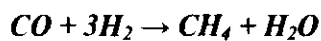
Some advantages of FT hydrocarbons compared to crude oil as a feedstock for fuel production are the absence of sulfur, nitrogen or heavy metal contaminants, and the low aromatic content (Steynberg, 2004, p. 1-63). The most important goal of FT technology is to utilize the abundant and low cost natural gas to produce “clean” in terms of low sulfur and low aromatic in middle distillates/fuels, with the main co-product is parafinic naphtha to be sold as steam cracker feedstock to make mainly ethylene and propylene. Moreover, other high value co-product such as detergent, synthetic lubricant, propylene and alpha olefins are used for production of polymers.

2.2 FT PRODUCT DISTRIBUTION

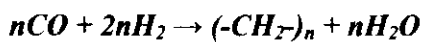
The depletion of fossil energy reserves and tremendous reserves of natural gas make the Fischer-Tropsch synthesis very attractive. Fischer-Tropsch synthesis (FTS) is expected as a production of method of liquid fuels instead of petroleum fuels.

In FTS, the synthesis gases which are CO and H₂ are converted to hydrocarbons mainly over Co or Fe based catalysts according to the following reactions (Steynberg, 2004, p. 198):

Methane,



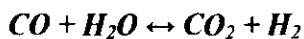
Heavier hydrocarbons,



Alcohols,



Water gas shift (WGS),



The synthesis gas feed can come from coal or residual oil gasification, methane reforming, or from biological wastes. There are also some renewed interests in recent years in FTS, especially for selective production of petrochemical feed stocks such as ethylene, propylene and butylenes. The mechanism of the FTS resembles a polymerization reaction where a monomeric unit is added to a growing hydrocarbon chain (Haghshenas, 2010).

Regardless of the operating conditions, FT reactions always produce a wide range of hydrocarbon and oxygenated hydrocarbon products. Methane, which is an unwanted product, will always present and its selectivity can vary from as low as about 1% up to 100%. At the other end of the product, the selectivity of long chain linear waxes can vary from zero to over 70%. Ruthenium which operates at about 170°C produces waxes

with carbon numbers in the polyethylene range. The same catalyst at about 400°C will produce mainly methane. The intermediate carbon number products between two extremes are only produced in limited amounts. Thus, for carbon atom basis, it is not possible to produce more than about 18% C₂, about 16% C₃, about 42% gasoline/naphtha (C₅ to 200°C boiling point) and about 20% diesel fuel (200 to 320°C) (Steynberg, 2004, p. 211).

The spread in carbon number products can be varied by altering the operating temperature, the type of catalyst, the amount or type of promoter present, the feed gas composition, the operating pressure, or the type of reactor used.

2.3 CATALYSTS FOR FT SYNTHESIS

Only for metals from group VIII metals, Fe, Co, Ni and Ru have sufficiently high activities for the hydrogenation of carbon monoxide to execute possible application in FTS. Of the four metals, ruthenium is the most active metal followed by iron, nickel and cobalt. The molecular average weight of hydrocarbons produced by FT synthesis decreased in the following sequence: Ru > Fe > Co > Rh > Ni > Ir > Pt > Pd. Thus only ruthenium, iron, cobalt, and nickel have catalytic characteristic which allow considering them for commercial production (Khodakov et al., 2007).

Although ruthenium is the most active, but its high cost and low worldwide reserves neglects it for a large scale industrial application. Nickel is also very active but it has two major disadvantages. Being a powerful hydrogenating catalyst it produces much more methane than Co or Fe catalysts. Nickel tends to form volatile carbonyls resulting in continuous loss of the metal at the temperatures and pressures at which practical FT plants operate (Khodakov et al., 2007). From the above explanation, it is clear that only cobalt and iron based catalyst can be considered as practical FT catalyst.

Table 2.1: Metal Cost for FT (Steynberg, 2004, p. 229)

Approximate relative cost of metals active for FT	
Fe	1
Ni	250
Co	1000
Ru	48000

**Fe as scrap metal*

Cobalt and iron are the metals which were suggested by Fischer and Tropsch as the catalyst for syngas conversion. Both cobalt and iron catalysts have been used in the industry for hydrocarbon synthesis. A brief comparison of cobalt and iron catalyst is shown in Table 2. From the table, cobalt catalysts are more expensive, yet they are more resistant to deactivation. Although the activity at low conversion of two metals is comparable, the productivity of at higher conversion is more significant with cobalt catalysts. Water generated by FT synthesis slows the reaction rate on iron to a greater extent than on cobalt catalysts. At relatively low temperatures (473 – 523 K), chain growth probabilities of about 0.94 have been reported for cobalt base and 0.95 for iron catalysts. The water-gas shift reaction is more significant to iron than on cobalt catalysts.

Iron catalysts usually produce more olefins. Both iron and cobalt catalysts are very sensitive to sulfur, which could poison them. For iron-based catalysts, the syngas should not contain more than 0.2 ppm of sulfur. For Co catalysts, the amount of sulfur in the feed should not exceed 0.1 ppm. Cobalt catalysts supported on oxide support are generally more resistant to attrition than iron coprecipitated counter parts which they are more suitable for use in slurry-type reactors. Iron catalyst produce hydrocarbons and oxygenated compounds under different pressures, H₂/CO ratios, and temperatures up to 613 K. Moreover, cobalt catalysts operate at a very narrow range of temperatures and pressures, which an incremental of pressure leads to a spectacular increase in methane selectivity. Iron catalysts seem to be more appropriate for conversion of biomass-derived syngas to hydrocarbons than cobalt systems because they can operate at lower H₂/CO ratios (Khodakov et al., 2007).

Table 2.2: Comparison between Cobalt and Iron Catalysts

Parameter	Cobalt Catalysts	Iron Catalyst
Cost	More expensive	Less expensive
Lifetime	Resistant to deactivation	Less resistant to deactivation (coking, carbon deposit, iron carbide)
Activity at low conversion	Comparable	
Productivity at high conversion	Higher; less significant effect of water on the rate of CO conversion	Lower, strong negative effect of water on the rate of CO conversion
Maximal chain growth propability	0.94	0.95
Water gas shift reaction CO + H₂O → + H₂	Not very significant; more noticeable at high conversion	Significant
Maximal sulfur content	<0.1 ppm	<0.2 ppm
flexibility (temperature and pressure)	Less flexible; significant influence of temperature and pressure on hydrocarbon selectivity	Flexible; methane selectivity is relatively low even at 613 K
H₂/CO ratio	~2	0.5-2.5
Attrition resistance	Good	Not very resistant

2.4 CARBON NANOTUBE SUPPORTER

Among all types of supports which are being used in heterogeneous catalyst, carbon materials have been a focus due to its particular characteristics which are [12]:

- Resistance to acid and base media
- Possibility to control the porosity and surface chemistry within certain limit
- Easy recovery of precious metal by support burning which results in low environmental effect

Two types of well known carbon materials are graphite nanofibers (GNF) and carbon nanotubes (CNT) (Serp et al., 2003). Among these two, CNT has become one of the most popular researches in nanoscience and nanotechnology due to their outstanding properties which make it versatile applications as polymer reinforcements for composites or breakthrough materials for energy storage, electronics and catalysis.

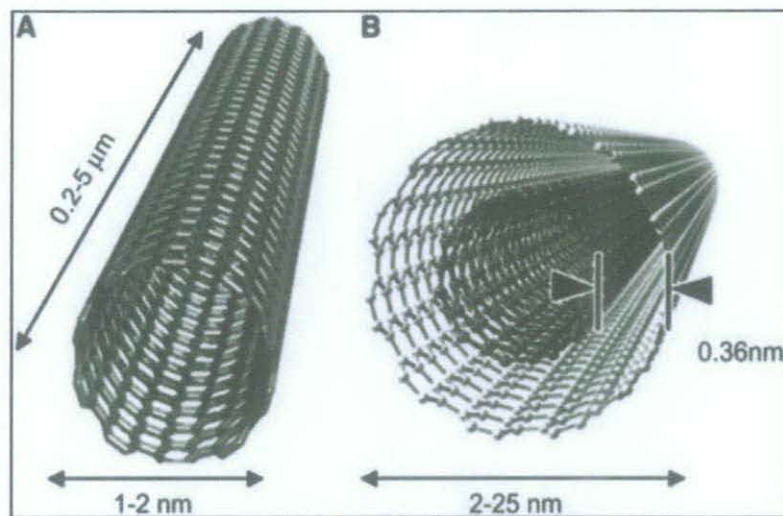


Figure 2.1: Carbon Nanotubes

Carbon nanotubes can be divided into two main categories which are SWNT and MWNT as shown in Figure 2.1. Basically, single-wall carbon nanotube are made of a perfect grapheme sheet like polyaromatic mono-atomic layer made of an hexagonal display of sp^2 hybridized carbon atoms that genuine graphite is built up with, rolled up into a cylinder and closed by two caps (semi-fullerenes). The internal diameter of these structures can vary between 0.4 and 2.5nm and the length range from few microns to several millimetres (Serp et al., 2003).

MWNT can be considered as concentric SWNT with increasing diameter and coaxially disposed. The number of walls can vary from two double wall nanotubes to several tens, so that the external diameter can reach 100nm. The concentric walls are regularly spaced by 0.34nm similar to the intergraphene distance evidenced in turbostratic graphite materials (Serp et al., 2003).

2.5 MICROEMULSION METHOD

2.5.1 Introduction

Basically, oil and water are not miscible and exist as water and oil phase, letting each of them saturated with traces of one another, if they are to be mixed. Emulsifier is a substance that is soluble in one or both solvents but will form a true molecular solution of emulsifier molecule monomer at low concentration. At higher concentration of emulsifier, they tend to combine into micelle particle. Emulsifier is a molecule that possesses both polar and nonpolar moieties. In diluted water (or oil) solution, emulsifier dissolves where it is present in homogeneous form. When the concentration of the emulsifiers exceeds the critical micelle concentration, the molecules of emulsifier spontaneously form aggregates micelles. Mixtures containing either three or four components mixture which are water, oil, emulsifier and coemulsifier are said to be kinetically and thermodynamically stable (Capek, 1999).

Microemulsion is defined as a system of water, oil and amphiphile (surfactant). At macroscopic scale, a microemulsion looks like a homogeneous solution but at molecular scale, the inside particles are heterogeneous (Eriksson et al., 2004). The different structures of a microemulsion at a given concentration are shown in the following figure:

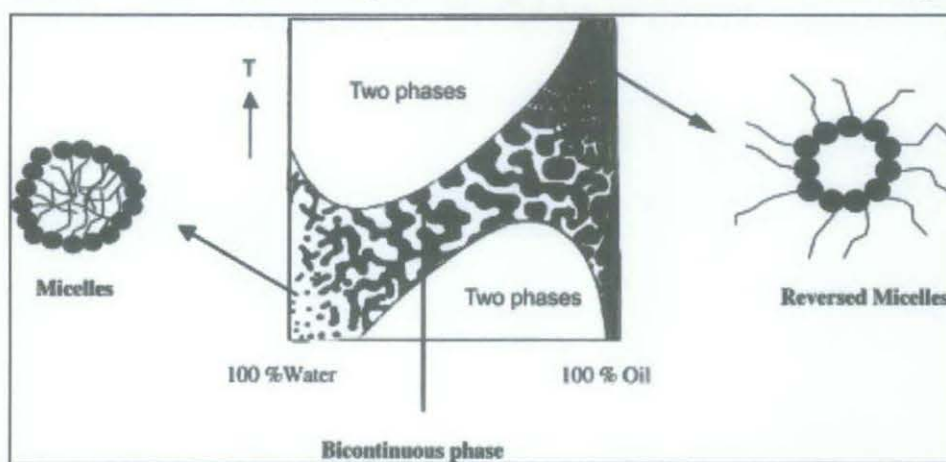


Figure 2.2: The microscopic structure of a microemulsion at a given concentration of surfactant as function of temperature and water concentration

The internal structure of a microemulsion at a given temperature is determined by the ratio of its components. At high concentration of water, the internal structure of a microemulsion consists of tiny oil droplets in a continuous water phase known as micelle. With increased oil concentration, a bicontinuous phase without clear form is produced. At high oil concentration, the opposite situation occurs where the bicontinuous phase transforms into structure of small water droplets in continuous oil phase known as reverse micelle or w/o microemulsion (Eriksson et al., 2004).

Microemulsion is an excellent media to assist chemical reactions. It has been reported that microemulsion can dissolve a large number of different compounds, acquire large internal interface as well as the ability to form spontaneously.

The size of droplets varies from 10 – 100nm depends on the type of surfactant. Note that this system is very sensitive towards the change of temperature, especially for non-ionic surfactant. As shown in the figure above, increasing the temperature will wipe out the oil droplets, while in the opposite way, reducing the temperature will wipe out the water droplets forming a two phase system (Eriksson et al., 2004).

2.5.2 Preparation of Nanoparticles

Reverse micelle or w/o microemulsion is the focus of the project. W/o microemulsion can be pictured as small compartments made up of hydrophilic part of the surfactant which is filled with water. At the center of the hydrophilic droplets, a certain amount of water-soluble material can be dissolved. An amount of precursor transition metal, for example will dissolve into the center before the final metal particle takes place.

Note that this system is highly sensitive to temperature due to the physical and chemical properties of the constituents. Thus, it is important to choose a proper temperature of

microemulsion system, which is stable at room temperature or at higher temperature, 70°C (Eriksson et al., 2004).

There are two main ways of preparation in order to obtain nanoparticles from microemulsion method:

- i) By mixing two microemulsions, one contains the precursor and the other the precipitating agent as shown in Figure (a).
- ii) By adding the precipitating agent directly to the microemulsion containing the metal precursor as shown in Figure (b).

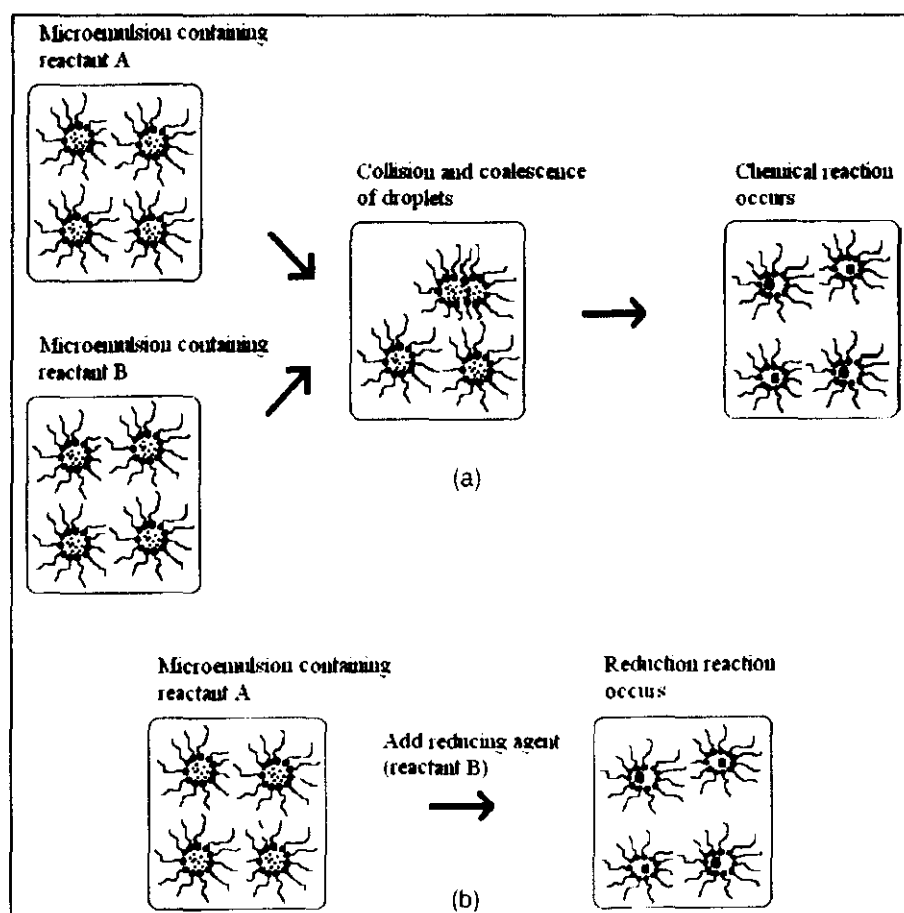


Figure 2.3: Modes of particle preparation from microemulsion: (a) Mixing of two microemulsion; (b) Direct addition of reducing agent to the microemulsion (Eriksson et al., 2004)

The following figure shows a clear picture of the steps of catalyst preparation:

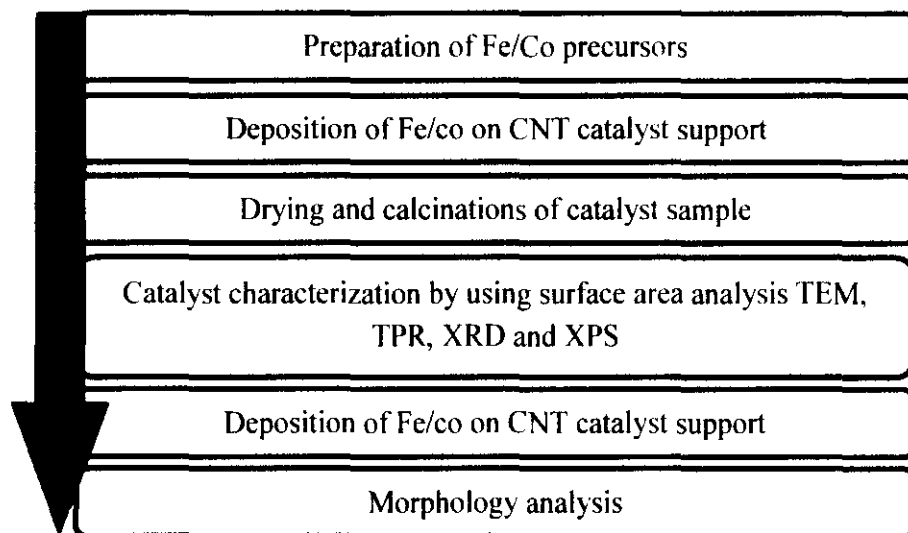


Figure 2.4: Principal Stages in the Preparation of Fe/Co Supported FT Catalyst (Khodakov et al., 2007)

The following descriptions explain about the general microemulsion procedure. This method consists of preparing two types of microemulsion.

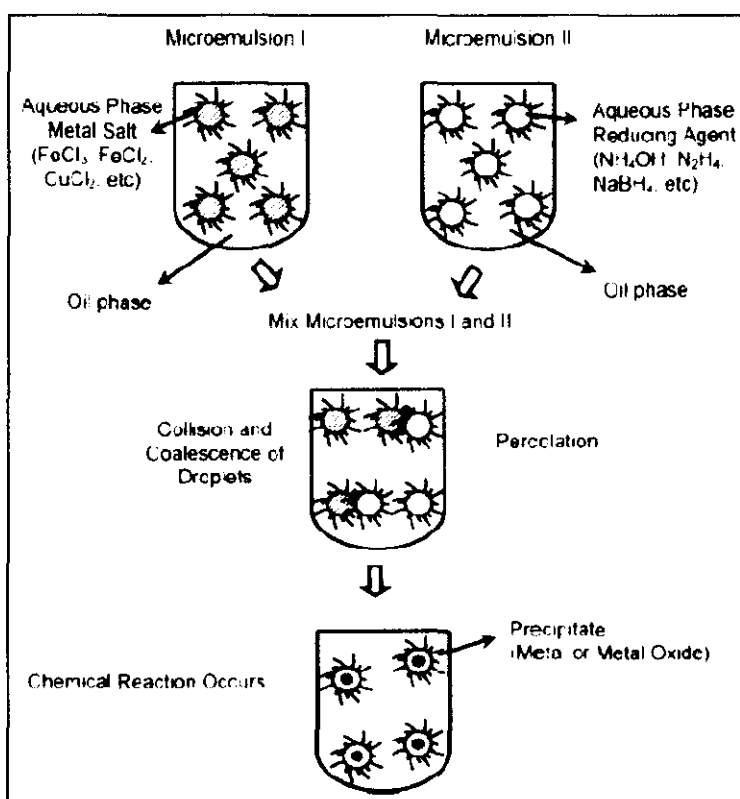


Figure 2.5: Principal stages of metal nanoparticle preparation using microemulsion
 The first microemulsion contains metal salt in the droplets, and the second microemulsion represents the reducing agent (NaBH₄, N₂H₄, etc.) located inside the

droplets. A series of iron and cobalt metal salt are dissolved in the aqueous phase which consists of four different ratio which are listed in Table. Then both microemulsions are mixed together. The metal salt inside the micelles is reduced to metallic particles by the reducing agent where by the rate of the reaction is controlled by the intermediate exchange rate.

The Fe/Co fine particles were prepared by using a H₂O/sodium di-2-ethylhexylsulfosuccinate (AOT)/isooctane ternary system. The Fe/Co- containing microemulsion is prepared by mixing the AOT in isooctane with an aqueous solution of cobalt chloride and iron chloride. The reducing microemulsion was obtained by mixing AOT isooctane with an aqueous solution of NaBH₄. Both emulsions are transparent. They are mixed which the color of the product turned from light pink to black in few seconds. The size of the produced Fe/Co metal particle is lower than 3nm (Khodakov, 2007).

2.5.3 Influence of Various Factors on the Particle Size

2.5.3.1 Size of the Water Droplets

The size of the resulted metal particle depends on the size of droplets in the microemulsion, whereas the size of the droplets is controlled by the water-to-surfactant ratio, ω . An increase ratio at constant concentration of surfactant will increase the diameter of the droplets. As reviewed by Lisiecki and Pileni, the size of Cu Nanoparticles prepared in a system consisting of AOT, cyclohexane and water increased from 2 to 10nm as ω changed from 1 to 10 (Eriksson et al., 2004).

2.5.3.2 Surfactant Concentration

While the amount of water and oil is fixed, the incremental of surfactant amount will increase the number of droplets, meaning that the number of metal ions per droplet will decrease and so the size of the particle.

Several studies have shown that the size of the droplets has a great influence on the size of the particles that are formed after precipitation of the precursor. However, there is not any direct correlation between the size of the droplets (10–100 nm) and the size of the obtained particles (Eriksson et al., 2004).

Formation of particles occurs in two steps. First the nucleation process inside the droplets and the next step is the aggregation process to form the final particle. The rate of particle growth is controlled by the presence of the surfactant which indirectly prevents the nuclei from growing too fast. As the result, the particle will grow at the same rate to form particles in homogeneous size distribution (Eriksson et al., 2004).

2.5.3.3 Nature of the Reducing Agent

Hydrazine is an effective reducing agent for transition metal salts. A fast nucleation process will result in the production of smaller particle. By increasing the concentration of hydrazine while the concentration of metal salt is unchanged, the particle size will decrease (Eriksson et al., 2004).

2.5.4 Advantages of Microemulsion Method

Metal particle size is one of the most important elements in the mechanism of CO hydrogenation, the reaction in Fischer-Tropsch process. As being studied,

microemulsion method owns several important advantages which distinguish this method from others:

- Ability to control metal particle size with a narrow particle size distribution, despite of the metal content (Trépanier et al., 2010).
- Ability to resize the size of metal particle formed in water-to-oil (w/o) by changing the water-to-surfactant ratio (Trépanier et al., 2010).
- Recent study shows that catalysts prepared by w/o microemulsion increase the rate of Co hydrogenation, H₂ chemisorption and C₂ selectivity (Trépanier et al., 2010).
- The activity of Fe/SiO₂ catalyst produced by microemulsion is better than the same catalyst produced by incipient wetness impregnation method (Trépanier et al., 2010).
- Bimetallic particle can be obtained at room temperature (Eriksson et al., 2004).
- No effect of the support on the formation of the particles (Eriksson et al., 2004).

2.6 CRITICAL MICELLE CONCENTRATION

Some molecules are said to own two distinct components which have different attraction in solution. Some molecules which have attraction to polar solutes, like water are hydrophilic, while the molecules which attracted to non-polar solutes, like hydrocarbons are said to be hydrophobic. Molecules which contain both types of components are called amphiphilic as shown in the following figure (“Critical micelle concentration,” n.d.).

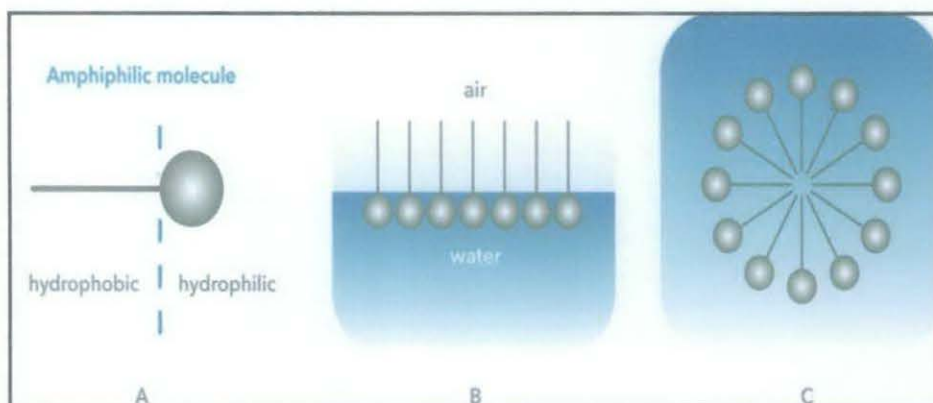


Figure 2.6: Amphiphilic Molecules (“Critical micelle concentration,” n.d.)

The polar side of the molecules tends to interact with water while the non-polar side avoids from interacting with water. There are two ways for such molecule to achieve both states. An amphiphilic molecule can arrange the polar side itself at the surface of the water while the non-polar will be held above the surface of the water either in air or non-polar fluid as shown in Figure (B). The presence of amphiphilic molecules on the surface disturbs the cohesive energy at the surface results in a lower surface tension. Such molecules are known as surfactant.

Another arrangement of amphiphilic molecules can let each component to interact with its favored surrounding. These molecules can form aggregate in which the hydrophobic portions are arranged within the cluster and hydrophilic sides are exposed to the solvent. Such formation of aggregate are known as micelle as shown in Figure (C).

The proportion of the micelle molecules in the bulk of liquid depends on the concentration of the amphiphile. At low concentration surfactant will favor arrangement on the surface. As the surface is filled with surfactant, more molecules will arrange into micelle. At some concentration the surface becomes completely filled with surfactant and further additions must be arranged as micelles. This type of concentration is known as Critical Micelle Concentration (CMC). The measurement of surface tension can be

used to find CMC. The graph of surface tension versus the log of concentration of surfactant is pictured as follows:

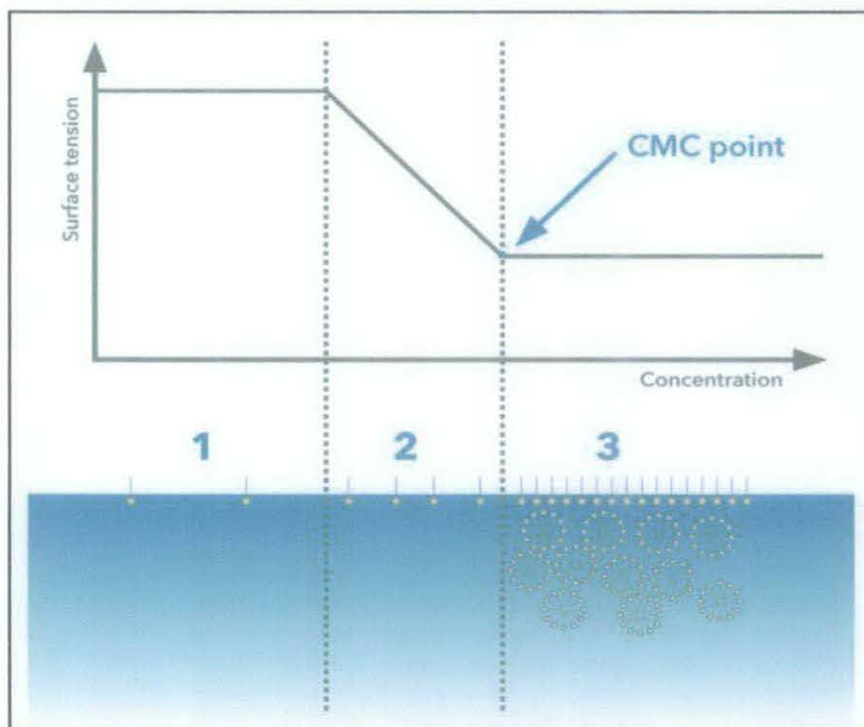


Figure 2.7: Critical Micelle Concentration (“Critical micelle concentration,” n.d.)

As viewed from the graph, there are three phase of concentration. In the first phase, at very low concentrations of surfactant, only slight change in surface tension occurs. Next, additional surfactant decreases the surface tension as shown in phase 2. As the concentration of surface exceed phase 2, surfactant becomes fully loaded results in no further change in surface tension (“Critical micelle concentration,” n.d.).

2.7 CATALYST ANALYSIS

In heterogeneous catalyst, frequently used catalysts are metal particles attached on the supporter. The size of metal particles plays an important role for the catalyst efficiency, whereas the determination of size distribution is one of the main tasks of electron microscopy in the catalyst. Listed below are the characterization methods that are used to analyze the sample of the catalyst.

2.7.1 Transmission Electron Microscopy Analysis (TEM)

TEM and Scanning Electron Microscopy (SEM) are related techniques that use high energy electron beam to image a sample. High energy electrons, incident on an ultra-thin sample allow for image resolutions that are on the order of 1 – 2 Angstroms. Compared to SEM, TEM has better resolution which capable of additional analytical measurements and requires more sample preparation (“Transmission Electron Microscopy (TEM) and Scanning Transmission Electron Microscopy (STEM),’ n.d.).

The TEM is also capable of forming a focused electron probe, as small as 20 Å, which can be positioned on very fine features in the sample for microdiffraction information or analysis of x-rays for compositional information. The latter is the same signal as that used for EMPA and SEM composition analysis, where the resolution is on the order of one micron due to beam spreading in the bulk sample. The spatial resolution for this compositional analysis in TEM is much higher, on the order of the probe size, because the sample is so thin. Conversely the signal is much smaller and therefore less quantitative. The high brightness field-emission gun improves the sensitivity and resolution of x-ray compositional analysis over that available with more traditional thermionic sources. Listed below are the ideal uses of TEM analysis (“Transmission Electron Microscopy (TEM) and Scanning Transmission Electron Microscopy (STEM),” n.d.):

- Identification of nm sized defects on integrated circuits, including embedded particles and residues at the bottom of vials.
- Determination of crystallographic phases as a function of distance from an interface.
- Nanoparticle characterization.
- Catalyst support coverage.

2.7.2 Field Emission Scanning Electron Microscopy Analysis (FESEM)

Under vacuum, electrons generated by a Field Emission Source are accelerated in a field gradient. The beam passes through Electromagnetic Lenses, focusing onto the specimen. As result of this bombardment different types of electrons are emitted from the specimen. A detector catches the secondary electrons and an image of the sample surface is constructed by comparing the intensity of these secondary electrons to the scanning primary electron beam. Finally the image is displayed on a monitor (“FESEM History and Principle.”, n.d.).

2.7.3 Energy Dispersive X-ray Analysis (EDX)

Energy dispersive x-ray analysis (EDX), also referred to EDS and EDAX, is an X-ray technique used to identify the elemental composition of a sample. The applications of EDX include materials and product research, trouble shooting, deformation and other.

EDX systems are usually attached to SEM instruments where the image capability of the microscope is used to identify the sample of interest. The data generated by EDX analysis comprise of spectra showing peaks corresponding to the elements making up the true composition of the sample being analyzed. In addition, the sample of interests can be examined in situ with little or no sample preparation.

2.7.4 Surface Area Analysis (BET)

A common method for determining total catalyst surface area is the BET method which uses nitrogen adsorption that applies to most heterogeneous catalysts and it is prone to change during preparation, conditioning and in use of high temperature. The changes occur during the catalyst life are mostly towards the loss of surface area. The physical adsorption of the gas over entire exposed surface of catalyst and the filling pores is

called physisorption and it is used to measure total surface area and pore size analysis of nanopores, micropores and mesopores.

The BET surface area measurement is the key in understanding the behavior of the catalyst, as the catalyst reacts with its environment via its surface. A higher surface area catalyst is more likely to react faster, dissolve faster and adsorb more gas than a similar catalyst with low surface area (Tavasoli et al., 2009; "BET surface Area & Gas Adsorption," n.d., "Determination of the surface area by the BET method," n.d.).

CHAPTER 3

METHODOLOGY

3.1 CALCULATION

As a part of methodology, several calculations were done before proceeding to any experiment in order to gain precise result. Most of the calculations were focused based on the items listed as the following.

3.1.1 Dilution of Nitric Acid for Purification of CNT

CNT has to be purified or regenerated to eliminate the impurities inside. Furthermore, the regeneration process will return its active form as catalyst supporter. Nitric acid is the chemical used for regenerating back the ability of CNT. The CNT has to undergo the preliminary step which is called purification treatment before it can be used as a supporter. Before introducing any amount of CNT into nitric acid (HNO_3), nitric acid has to be diluted. In the lab, 65% volume of HNO_3 is provided whereas the appropriate volume to treat the CNT is 35% volume. *Appendix 3.1* shows a detail calculation on this part.

3.1.2 Amount of Iron and Cobalt Nitrate for Catalyst Preparation

There are four samples to be experimented in the project which are 100Co/CNT, 90Co10Fe/CNT, 80Co20Fe/CNT and 70Co30Fe/CNT. For each composition, mass basis is used to determine the amount of metal in the catalyst. Note that, the chemicals available for both metals are in nitrate form. The detail calculations are shown in *Appendix 3.2*. Below is the amount of metal for each catalyst:

Table 3.1: Appropriate Amount of Metals

No.	Samples			
	1	2	3	4
Composition	Co: Fe (100:0)	Co : Fe (90:10)	Co : Fe (80:20)	Co : Fe (70:30)
Amount of Cobalt Nitrate	0.12g	0.11g	0.098g	0.086g
Amount of Iron Nitrate	-	0.018g	0.0367g	0.0541g
Net Total	0.12g	0.128g	0.1347g	0.1401g

3.1.3 Molarity of Triton X-114 in Cyclohexane

Triton X-114 acts as the surfactant which enables the mixing of oil and water. The oil phase for the microemulsion is cyclohexane. An appropriate amount of surfactant is used to result in homogenous form. The solution of cyclohexane, water and surfactant which produce the clearest solution will be chosen as the best homogeneous mixture. Base on previous report, the most suitable molarity of Triton X-114 in the cyclohexane is 0.2molar. For 0.2molar of Triton X-114, 100ml of cyclohexane is used. Base on calculation which is shown in *Appendix 3.3*, the mass of Triton X-114 is 11.175g_{Triton}.

3.1.4 Ratio of Water-Surfactant

Ratio of water and surfactant is varies from 3 to 10. A detail calculation is shown on the determination of ratio of water to surfactant is shown in *Appendix 3.4*. The ratio is made base on mol basis as shown in the following table:

Table 3.2: Volume of Water for Applied Amount of Surfactant

No.	Ratio of Water-Surfactant							
	1	2	3	4	5	6	7	8
Ratio	3:1	4:1	5:1	6:1	7:1	8:1	9:1	10:1
Mol of Triton X-114	0.02	0.02	0.02	0.02	0.02	0.02	0.02	0.02
Mass of Water	1.08g	1.44g	1.80g	2.16g	2.52g	2.88g	3.24g	3.60g
Volume of Water	1.08ml	1.44ml	1.80ml	2.16ml	2.52ml	2.88ml	3.24ml	3.60ml

3.1.5 Amount of Hydrazine

Another chemical which is added into each sample is Hydrazine (N_2H_2). Hydrazine is added into each sample solution to improve the metal nanoparticle formation in the core of water micelles by reducing iron oxide and cobalt oxide. A detail calculation is shown on the determination of ratio of water to surfactant is shown in *Appendix 3.5*. Hydrazine is inserted in excess at a ratio of 10:1 (hydrazine-Fe/Co) in each sample as shown in the following table:

Table 3.3: Amount of Hydrazine versus Fe/Co

No.	Samples			
	1	2	3	4
Total amount of Co and Fe Nitrate	0.12g	0.128g	0.1347g	0.1401g
Total mol of Co and Fe Nitrate	0.002	0.0022	0.0023	0.0024
Ratio	10:1	10:1	10:1	10:1
Amount of Hydrazine	0.641g	0.7051g	0.7372g	0.77g

*Note that the molecular weight of hydrazine is 32.05g/mol.

3.2 PREPARATION OF CO/Fe CATALYSTS

As being studied (Khodakov et al., 2007; Trépanier et al., 2010; Eriksson et al., 2004), the methodology of catalyst preparation for laboratory scale for reverse microemulsion method is explained as follows:

1. Mknano-MWCNT (>95%) is treated with 30 wt.% HNO_3 at $100^\circ C$ for overnight, and it is washed deionized water. It is dried at $120^\circ C$ for 6 hours.
2. Co/Fe particle is prepared in a reverse microemulsion by using a nonionic surfactant Triton X-100 (Aldrich) and cyclohexane (C_6H_{12}) as the oil phase.
3. Four (4) samples of Fe/Co composition are prepared by using aqueous cobalt nitrate ($Co(NO_3)_2 \cdot 6H_2O$) 5 wt.% (Merck) and iron nitrate ($Fe(NO_3)_3 \cdot 9H_2O$) 5 wt.% (Merck) as shown as follows:

Table 3.4: Composition of Fe VS Co

No. of Sample	Composition of Co/Fe (5 wt. %)
1	100 : 0
2	90 : 10
3	80 : 20
4	70 : 30

4. Water-to-surfactant ratio is varied from 3 to 10.
5. The mixture is stirred vigorously until a microemulsion mixture is obtained (after 15 minutes).
6. Hydrazine is added in excess (hydrazine/(Fe/Co) = 10) to improve Fe/Co nanoparticle formation in the core of micelles by reducing iron oxide and cobalt oxide.
7. Appropriate purified CNT is added into the stirred solution.
8. During 3 hours of stirring, dropwise of tetrahydrofurane (THF), an emulsion destabilizing agent is added into the solution at 1ml/min by using a syringe pump. A fast addition could lead to fast particle agglomeration and uncontrolled particle deposition on the CNT support.
9. The mixture is left to settle slowly for overnight and decant it.
10. The solid sample of the catalyst is recovered by using vacuum filtration using ash less 90mm Ø x 100mm circle filtration paper (Whatman®) and wash several times with ethanol.
11. Remaining traces of surfactant and nitrates are removed by calcining the catalyst under nitrogen flow at 370°C for 3 hours and the catalyst is exposed to oxygen atmosphere during the cooling step.

3.3 PROJECT ACTIVITIES

Basically, the progression of Final Year Project 2 from week to week until **Week 8** is elaborated in the following table. Each job is done accordingly to avoid redundancy.

Table 3.5: Weekly Work Progression

Week	Work Progression	Assist/Action by
1	<ul style="list-style-type: none"> • Apparatus and equipment were collected from technician to run experiment with regards to purification of carbon nanotubes (CNT). • Meeting with master and PhD students to gain better understanding about the overall experiment. • All experiments with regard to reverse microemulsion were carried out at Block 3, Level 2. 	<ul style="list-style-type: none"> • Ms. Aisyah (Master Student – Ionic Liquid Laboratory) • Mr. Ali Khan (PhD Student – Block 1) • Mr. Firdaus (Technician – Block 5)
2	<ul style="list-style-type: none"> • Preparation of purified CNT was commenced. First batch containing approximately 3g of CNT managed to be prepared. • The purified CNT was distilled with HNO₃ for overnight before undergoing washing process with deionized water. • 10 washing were done for the purified CNT. • The traces of purified CNT were dried in an oven at 120°C for 5 hours. • The purified CNT was contained in the bottle for catalyst preparation. 	<ul style="list-style-type: none"> • Mr. Ali Khan (PhD Student – Block 1)
3	<ul style="list-style-type: none"> • Second batch of CNT containing 3g of CNT was prepared. • The washing and drying steps were done equally as in Week 2. • 7 washing were done for the purified CNT. 	<ul style="list-style-type: none"> • Mr. Ali Khan (PhD Student – Block 1)
4	<ul style="list-style-type: none"> • Apparatus and equipment were collected from technician to run experiment with regards to reverse microemulsion method. • Chemicals to run reverse microemulsion experiment were collected from Ms. Aisyah. • Experiment was carried out at Block 3, Level 2. • Meeting with Ms. Aisyah with regards to the choice of molarity of Triton X-114 inside cyclohexane. 	<ul style="list-style-type: none"> • Ms. Aisyah (PhD Student – Ionic Liquid Laboratory) • Mr. Ali Khan (PhD Student – Block 1) • Mr. Asnizam (Technician – Block 3)
5	<ul style="list-style-type: none"> • The ratio between water and surfactant is tested to find the best critical micelle concentration. The ratio of water-surfactant is varied from 3 to 8 at 2 molarity of Triton X-114 (surfactant) inside cyclohexane (oil phase). The best ratio of water-surfactant is 3-1. • Preparation of 4 samples of Fe/Co in different composition was proceed. The compositions are listed in <i>Table 3.1</i>. The samples were decanted 	<ul style="list-style-type: none"> • Ms. Aisyah (Master Student – Ionic Liquid Laboratory) • Mr. Ali Khan (PhD Student – Block 1)

	overnight. Only two samples managed to be prepared due to time constraint.	
6	<ul style="list-style-type: none"> • Preparation of another two samples of Fe/Co was continued. • After the samples had been decanted, all of them were dried in the oven for 5 hours at 120°C. • The samples were arranged in containers for calcinations. 	<ul style="list-style-type: none"> • Ms. Aisyah (Master Student – Ionic Liquid Laboratory) • Mr. Ali Khan (PhD Student – Block P)
7	<ul style="list-style-type: none"> • Four samples of Fe/Co nanocatalyst were calcined in Nanotechnology Lab for 5 hours, consisting of 1 hour start up of tubular furnace, 3 hours of calcinations and 1 hours of cooling down. • Transmission Electron Microscopy (TEM) was performed on the samples in Centralized Analytical Lab after the calcinations process. • The result of TEM was obtained on the next day. • Meeting with several technicians to book date for other characterization method (FESEM, XPS, TPR, BET) 	<ul style="list-style-type: none"> • Mr. Rosli (Technician – Nanotechnology Lab) • Mr. Idrus (Technologist)
8	Submission of Progress Report	<ul style="list-style-type: none"> • Dr. Lukman (FYP Coordinator)
9	Catalyst characterization via Field Emission Scanning Electron Microscopy (FESEM) and Energy Dispersive X-ray Spectroscopy (EDX).	<ul style="list-style-type: none"> • Mr. Anwar (Technologist – Centralized Analytical Lab)
10	Catalyst characterization via Temperature Programmed Reduction (TPR).	<ul style="list-style-type: none"> • Mr. Asnizam (Technician – Block 3)
11	Testing samples of catalyst in a microreactor.	<ul style="list-style-type: none"> • Mr. Ali Khan (PhD Student)
12	<ul style="list-style-type: none"> • Catalyst characterization via surface area analysis (BET). • Poster presentation 	<ul style="list-style-type: none"> • Mr. Omar (Technician – Centralized Analytical Lab)
13	Submission of softcopy and softbound of dissertation.	<ul style="list-style-type: none"> • Dr. Lukman (FYP Coordinator)

3.4 KEY MILESTONE/GANTT CHART

The important dates regarding to FYP 2 are listed in *Table 3.6*:

Table 3.6: Important Date

No.	Items	Date
1	Submission of Progress Report	14/11/2011
2	Poster Exhibition/Pre-SEDEX	5 – 6/12/2011
3	SEDEX	13/12/2011
4	Oral Presentation/Viva	27 – 30/12/2011
5	Submission of Hardbound	6/1/2012

CAB 4614 FINAL YEAR PROJECT 2 (FYP 2), Sept 2011**Timeline of Proposed Activities, Milestones and Deadlines****Project Title:** *Synthesis of Iron-Cobalt Nanocatalyst via Reverse Microemulsion Method***Supervisor:** *AP. Dr. Noor Asmawati Bt M Zabidi***Table 3.7: Proposed Gantt Chart**

No.	Detail/Week	1	2	3	4	5	6	7	8	9	10	11	12	13	14	15	
1	Project Work Continues	■															
2	Submission of Progress Report								■								
3	Project Work Continues								■								
4	Pre-SEDEX											■					
5	Submission of Draft Report												■				
6	Submission of Dissertation (soft bound)													■			
7	Submission of Technical Paper														■		
8	Oral Presentation															■	
9	Submission of Project Dissertation (hard bound)																■

3.5 TOOLS/EQUIPMENTS/CHEMICAL REQUIRED**Table 3.8: Tools/Equipments/Chemicals for FYP**

Tools/Equipments	
<ul style="list-style-type: none"> Laboratory Equipment for TEM, FESEM, EDX and BET Microreactor Shringe Pump Volumetric Flask 	<ul style="list-style-type: none"> Magnetic Stirrer Heater Whatman® Filtration Paper Membrane filter
Chemicals	
<ul style="list-style-type: none"> Mknano-MWCNT (>95%) 65% volume of HNO₃ Triton X-114 (Aldrich) Cyclohexane (Co(NO₃)₂).6H₂O 5wt.% (Merck) 	<ul style="list-style-type: none"> (Fe(NO₃)₃).9H₂O 5wt.% (Merck) Hydrazine Tetrahydrofurane Deionized Water Ethanol

CHAPTER 4

RESULT AND DISCUSSION

4.1 DATA GATHERING AND ANALYSIS

4.1.1 Determination of Water-To-Surfactant Ratio

Before introducing an amount of CNT inside surfactant solution, the best ratio of water-surfactant has to be determined first. As being studied, there are several possible ratios of water-surfactant which can make a homogenous oil-to-water microemulsion solution. The most homogenous solution will form a well mixed solution of oil and water without separating layer. The possible ratios of water to surfactant vary from 3 to 10 and the concentration of surfactant in oil phase is fixed at constant amount. At the beginning of the experiment, several ratios have been tested to observe the homogeneity of the microemulsion solution. Base on the experiment, below are the images of ratio water to surfactant from 6 to 8 at 0.2molar of surfactant concentration:

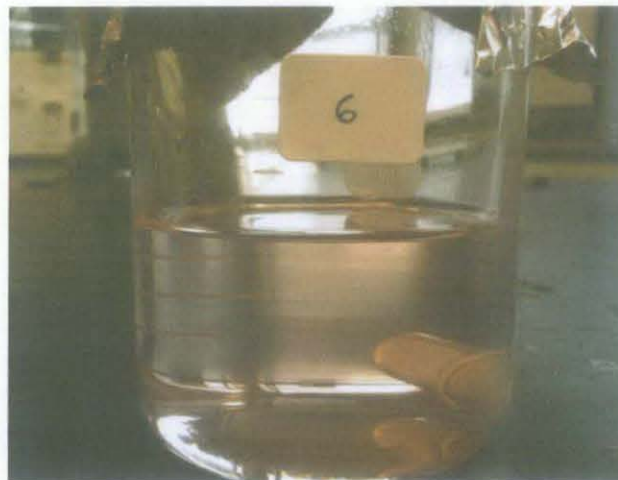


Figure 4.1: Water to surfactant (6 : 1)

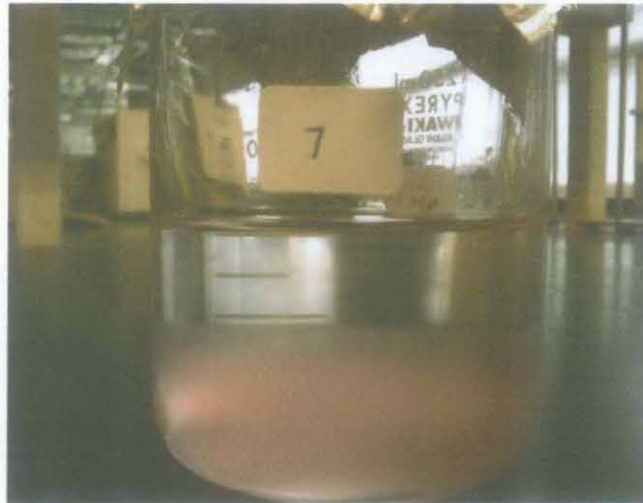


Figure 4.2: Water to surfactant (7 : 1)

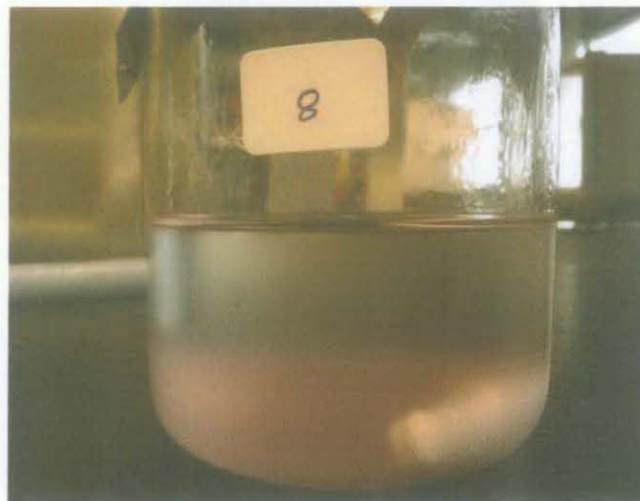


Figure 4.3: Water to surfactant (8 : 1)

As being observed, two layers of water and oil are formed at ratio of 7 : 1 which means at this particular ratio, the solution is no longer homogenous. At ratio 8 : 1, an equivalent result as ratio 7 : 1 is obtained. The ratio of 9 : 1 and 10 : 1 are not tested, assuming the result will be as equal as ratio of 7 : 1 and 8 : 1. As being experimented, the ratio of water to surfactant at 3 : 1 gives the best result where the solution of oil and water forms a well-mixed solution indicated by the lucidity of the solution as compared to ratio 4 : 1, 5 : 1 and 6 : 1.

When a sufficient amount of Triton X-114 dissolve in oil phase (cyclohexane) to form reverse microemulsion, several bulk solution properties of the oil change, particularly the surface tension, which decreases and the ability of the solution to dissolve water, is increasing. These changes will not occur until a minimum bulk concentration of Triton X-114 is reached. This type of concentration is called the critical micelle concentration (CMC).

As referred to the experiment, as the ratio of mol of water against surfactant is increased from 3 to 10, the reverse microemulsion solution will form a visible solution containing two separated layer, namely cyclohexane and water phase. As the water ratio is getting close to 6, visible sedimentation layer formed below a clear color solution. As cyclohexane has a lighter density than water, it will form above the solution, while another layer containing uniform mixture of cyclohexane, Triton X-114 and water will form under.

From the experiment, ratio of 3 : 1 (water-to-surfactant) is chosen as it forms the most clear and uniform solution. The clearer the mixture of three main elements namely cyclohexane, surfactant and water, the smaller micelles size are formed. In addition, the micelles or droplet act as a batch reactor to permit the attachment of metals on the CNT surface. As from the experiment, the ratio of 3: 1 (water-to-surfactant) is best suited with 0.2 molarity of Triton X-114 in cyclohexane which forms a homogenous solution at its critical micelle concentration.

4.2 ANALYSIS ON CHARACTERIZATION METHODS

4.2.1 Particle Size Distribution

As being discussed in **Chapter 2**, TEM is used to zoom into the smallest part of the catalyst. Below are the images which are taken with TEM:

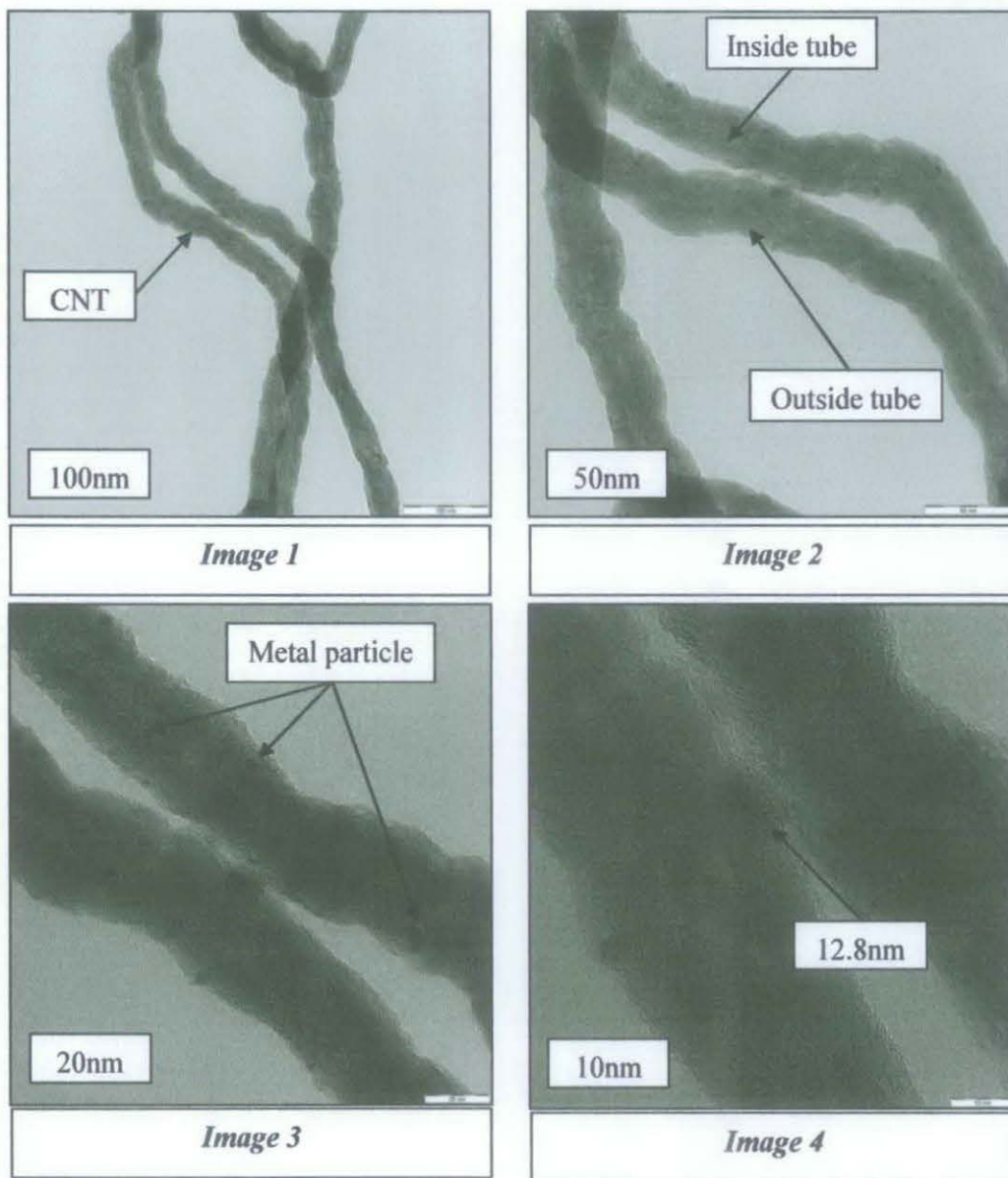


Figure 4.4: TEM images of 100Co/CNT at different magnification

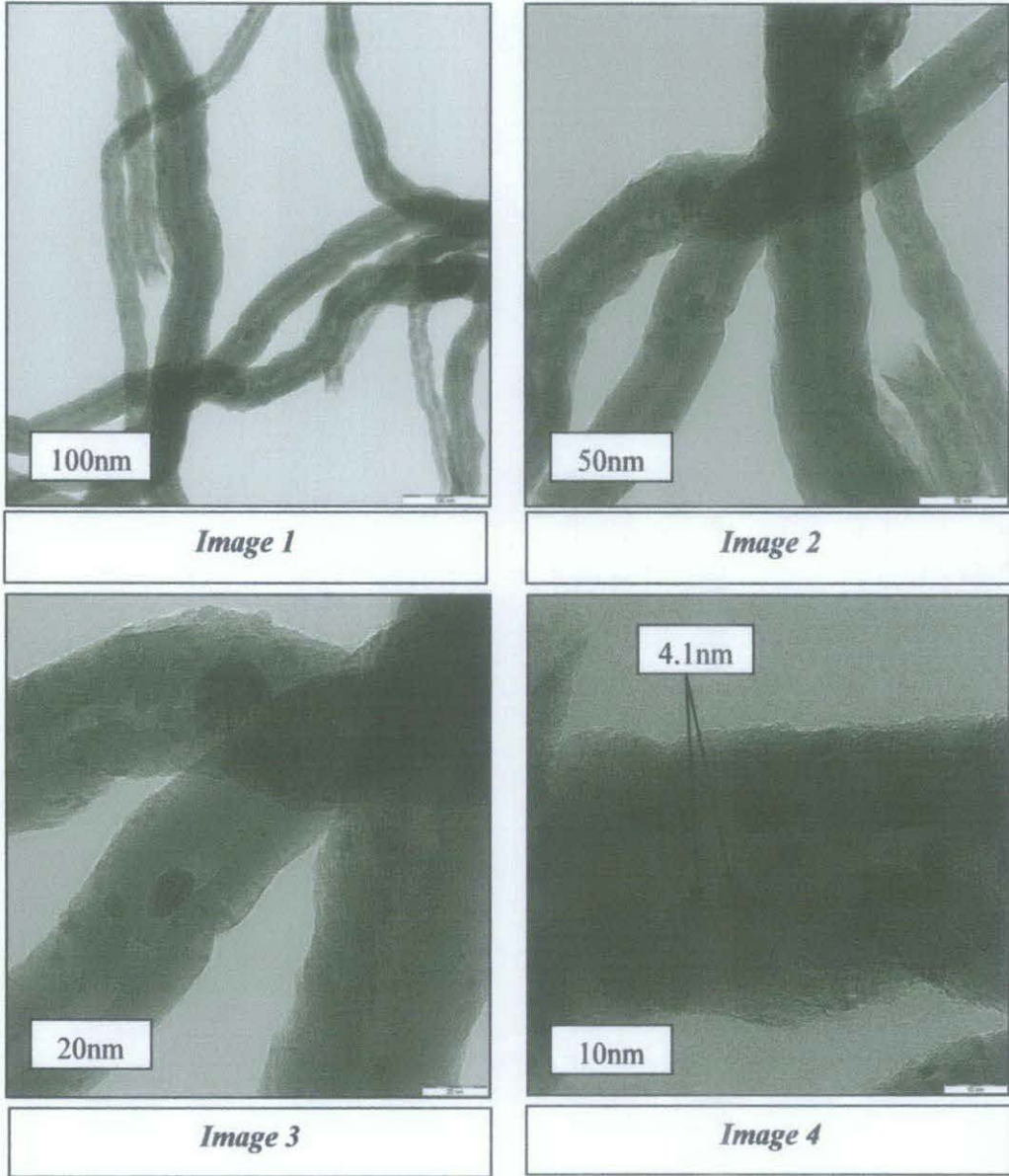


Figure 4.5: TEM images of 90Co10Fe/CNT at different magnification

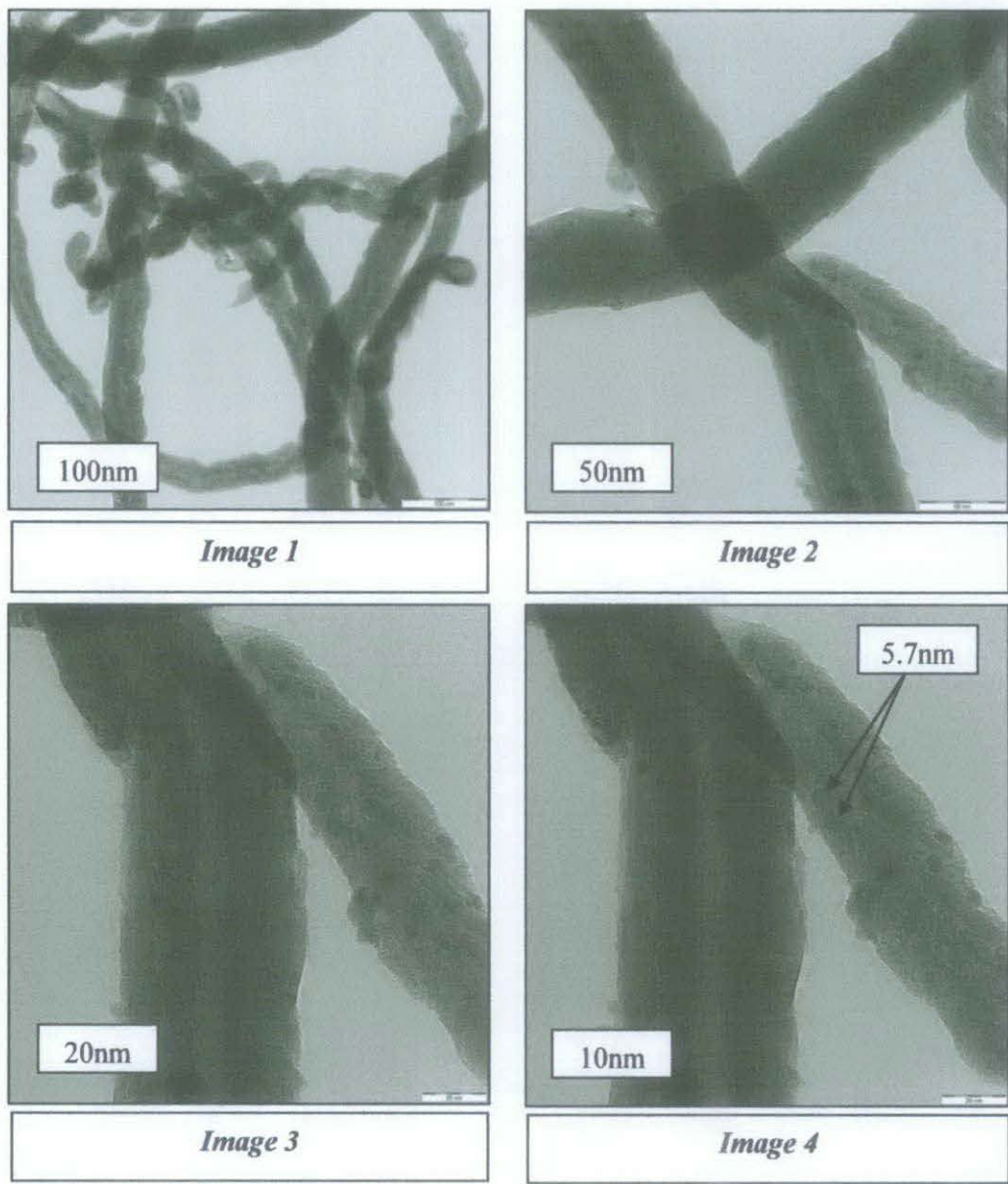


Figure 4.6: TEM images of 80Co20Fe/CNT at different magnification

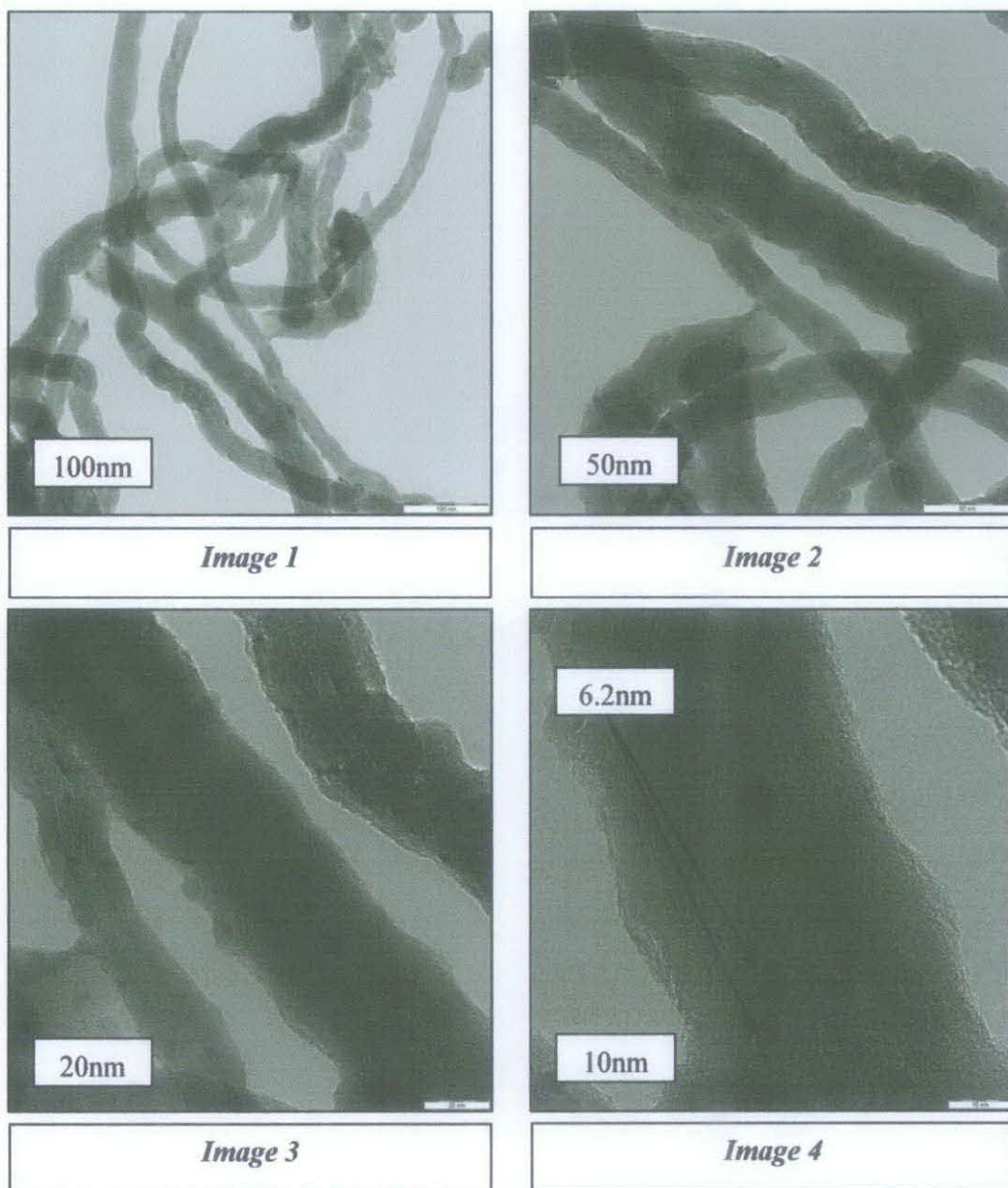


Figure 4.7: TEM images of 70Co30Fe/CNT at different magnification

The main purpose of TEM analysis is to analyze the metal particle size attach outside and inside the CNT surface area. The images show the particle distribution at different magnification. After some calculation, a clear particle size distribution for each composition is shown in the following bar chart:

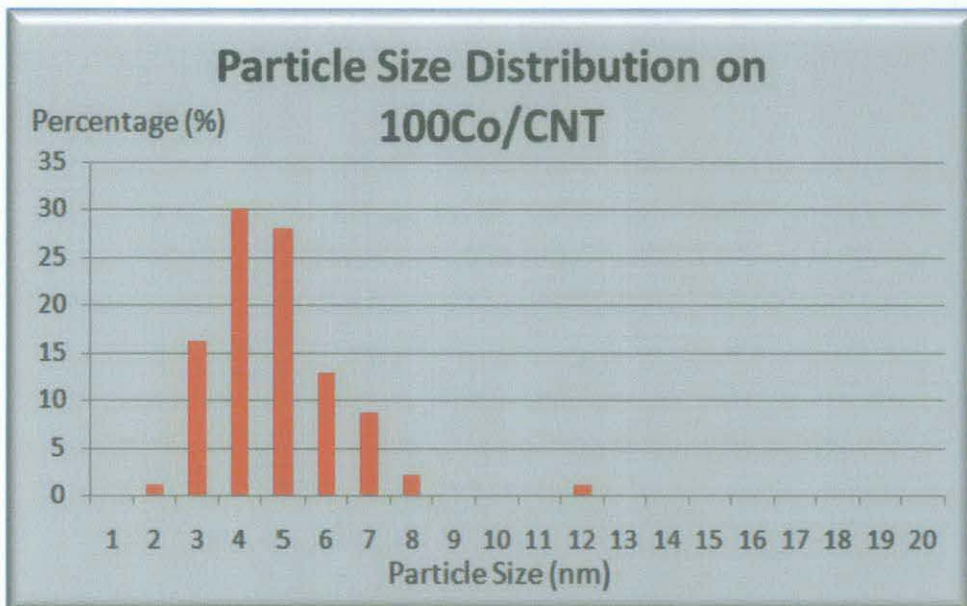


Figure 4.8: Metal distribution of pure cobalt catalyst

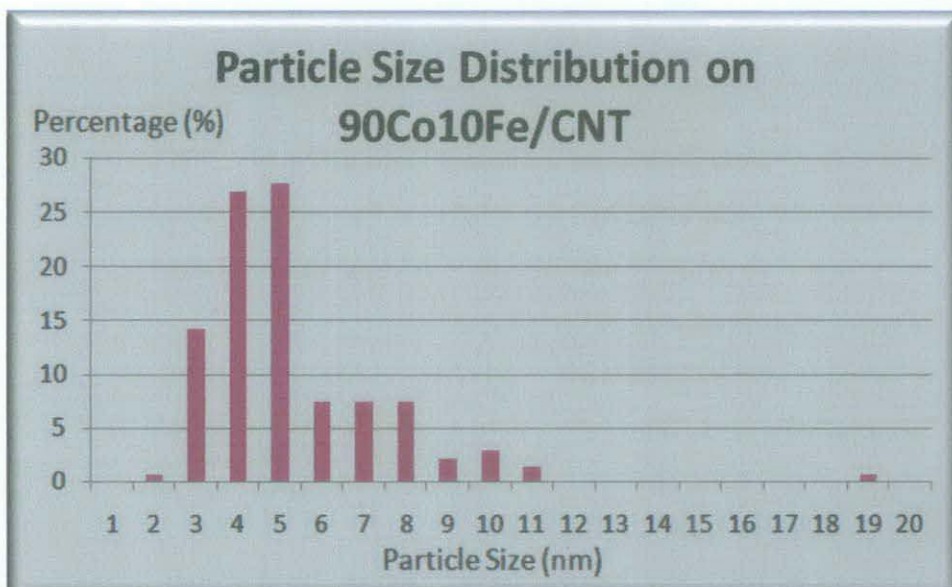


Figure 4.9: Metal distribution of 90Co10Fe/CNT

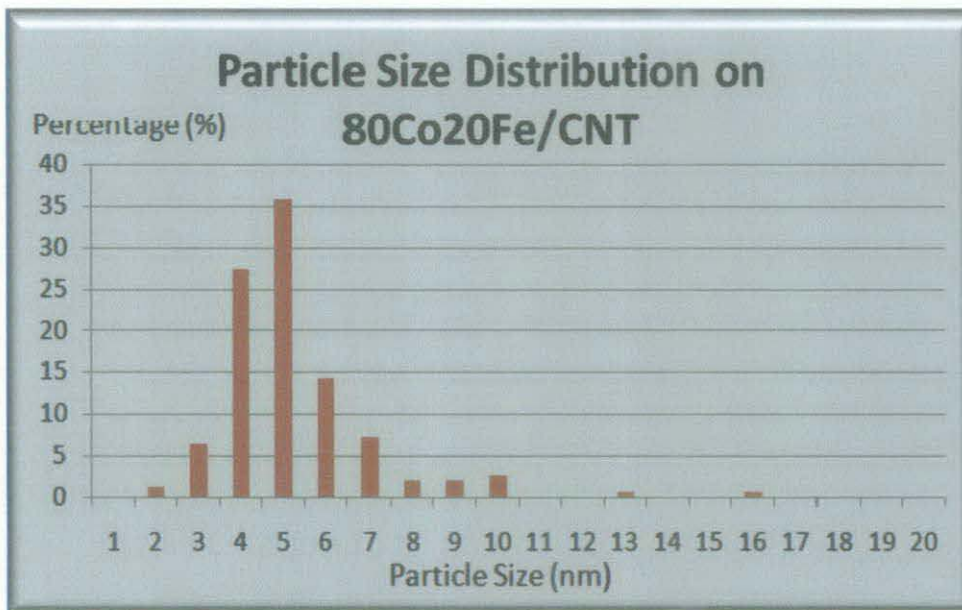


Figure 4.10: Metal distribution of 80Co20Fe/CNT

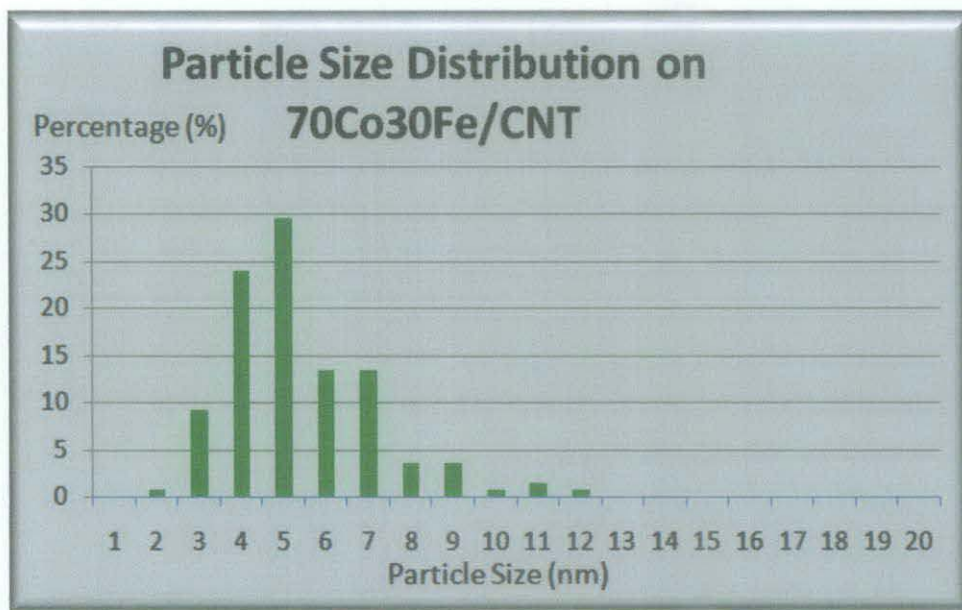
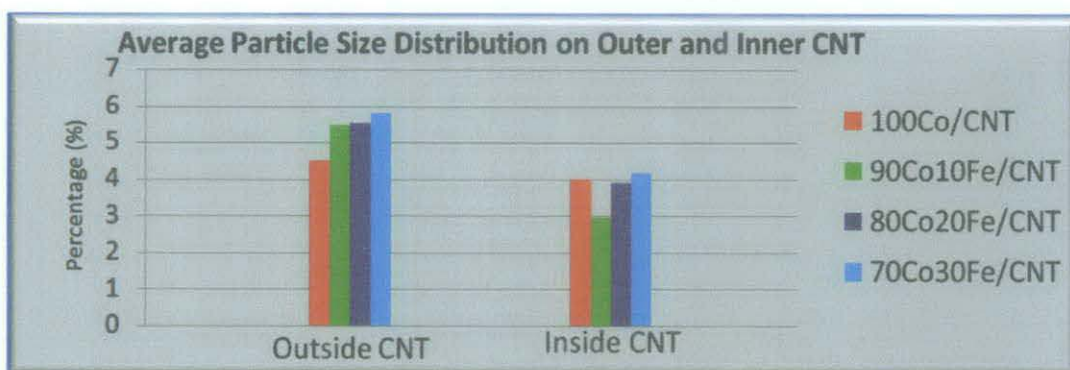


Figure 4.11: Metal distribution of 70Co30Fe/CNT



Composition	Average Outside Particle Size	Average Inside Particle Size
100Co/CNT	4.4nm	3.9nm
90Co10Fe/CNT	5.4nm	2.9nm
80Co20Fe/CNT	5.5nm	3.8nm
70Co30Fe/CNT	5.8nm	4.1nm

Table 4.1: Average particle size distribution for inner and outer surface of CNT

Composition	Average Particle Size	Population Standard Deviation
100Co/CNT	4.6nm	5.4nm
90Co10Fe/CNT	5.1nm	4.5nm
80Co20Fe/CNT	5.0nm	4.2nm
70Co30Fe/CNT	5.2nm	4.3nm

Table 4.2: Overall average particle size and standard deviation

As being shown by *Figure 4.8, 4.9, 4.10 and 4.11*, 80Co20Fe/CNT has the smallest mean average metal size and population standard deviation, 5.0nm and 4.2 respectively. As being observed from TEM images, most of the particles are distributed outside the CNT with an average size of 5nm whereas the inside particle is distributed with an average size of 3nm. Theoretically, the narrowest particle size could lead to a better performance and base on the result, 80Co30Fe catalyst has the most uniform metal distribution.

A rough idea that can be made through the analysis is the addition of iron in the catalyst could change the particle size in term of outside and also inside the nanotube. The more amount of iron added, the bigger the size of metal particle. A useful theory that can be made through the analysis is the smaller the population standard deviation of the metal particle, the better the efficiency and performance of the catalyst. A detail calculation from this part is emphasized in *Appendix 4.3*.

4.2.2 Surface Morphology and Element Composition

While TEM analysis can penetrate into the size of metal, the FESEM analysis provides a useful overview of the catalyst. One of the advantages of FESEM is it can detect the type of metal particle which is attached on the CNT. In addition, it can indicate the size of the metal particle. One of the disadvantages of FESEM is the system cannot penetrate into the inner surface of CNT to display the distribution of metal inside the CNT. The images obtained from FESEM are displayed as below:



Figure 4.12: FESEM images of 100Co/CNT

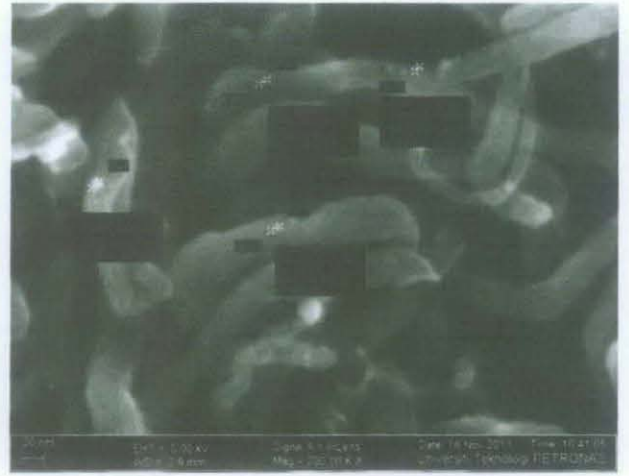


Figure 4.13: FESEM images of 90Co10Fe/CNT



Figure 4.14: FESEM images of 80Co20Fe/CNT



Figure 4.15: FESEM images of 70Co30Fe/CNT

Composition	wt% Element		
	Fe	Co	O
100Co/CNT	-	1.67	2.876
90Co10Fe/CNT	0.23	1.12	3.95
80Co20Fe/CNT	0.28	1.56	4.71
70Co30Fe/CNT	0.35	2.02	4.89

Table 4.3 Weight percentage of element on nanocatalyst

As being shown, the FESEM images do not provide significance information as it is hard to evaluate the distribution of metal particle. The result from Table 4.3 signifies the percentage of element exist on the nanocatalyst. As the amount of iron increases, the amount of metal oxide also increases.

4.2.3 Energy Dispersive X-ray Spectroscopy (EDX) Analysis

EDX is an analytical technique used for the elemental analysis or chemical characterization of a sample. It also provides useful information of the distribution of bimetallic on the catalyst surface area, specifically the distribution of CNT, cobalt and iron. The electron images and spectrum processing images from EDX are displayed in *Appendix 4.1* and *Appendix 4.2*.

4.2.4 Texture Properties of Nanocatalyst

BET analysis represents the surface area of the nanocatalyst. The largest surface area indicates a smaller size metal distribution on the catalyst hence favoring a better reaction. Displayed below is the result from BET which represents the nanocatalyst surface area:

Composition	Bet Surface Area (m ² /g)	Pore Volume (cm ³ /g)	Pore Diameter (Å)
100Co/CNT	145.45	0.45	115.67
90Co10Fe/CNT	119.63	0.46	130.56
80Co20Fe/CNT	121.34	0.46	128.32
70Co30Fe/CNT	130.24	0.46	125.48

Table 4.4: Properties of the catalysts

From *Table 4.4*, 100Co/CNT has the largest BET surface area. An addition of iron in the catalyst reduces the surface area and increases as the amount of iron increases. In term of pore diameter, 100Co/CNT has the lowest. Addition of iron will increase the pore diameter at the beginning and decreases as the amount of iron is becoming higher. Theoretically, the largest surface area can provide a better reaction between the nanocatalyst and the reactant.

4.2.5 Fischer-Tropsch Performance

The most important information is the Fischer-Tropsch performance which is provided by the microreactor. Shown in Figure 4.12 is the percentage of CO conversion and product distribution for each nanocatalyst.

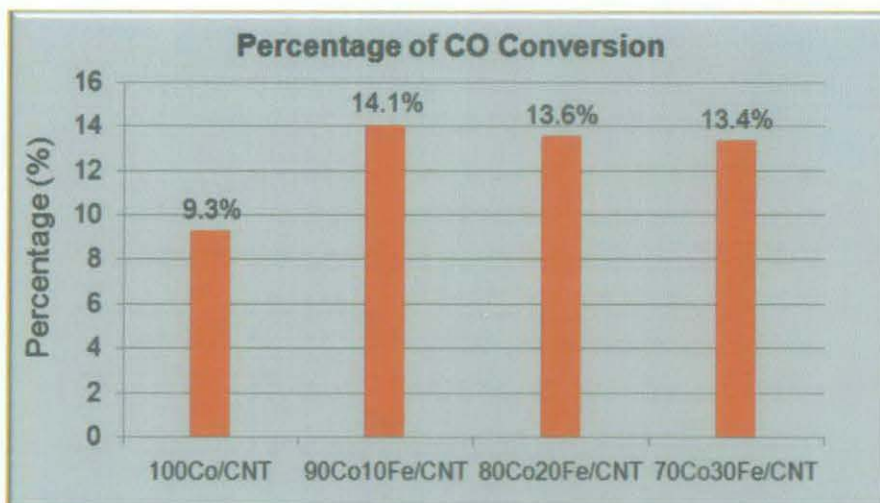


Figure 4.16: Percentage of CO conversion at different composition

From *Figure 4.16*, the highest conversion is given by 90Co10Fe/CNT which is 14.1% and the lowest conversion is given by 100Co/CNT. However, the difference percentage of CO conversion for 80Co20Fe/CNT and 70Co30Fe/CNT is only 0.2%. In addition, the CO conversion is increasing by adding some Fe into the pure Co catalyst. From the result, it can be hypothesized that an amount of Fe is needed to improve CO conversion and at the same time, increasing the amount of Fe could decrease the conversion.

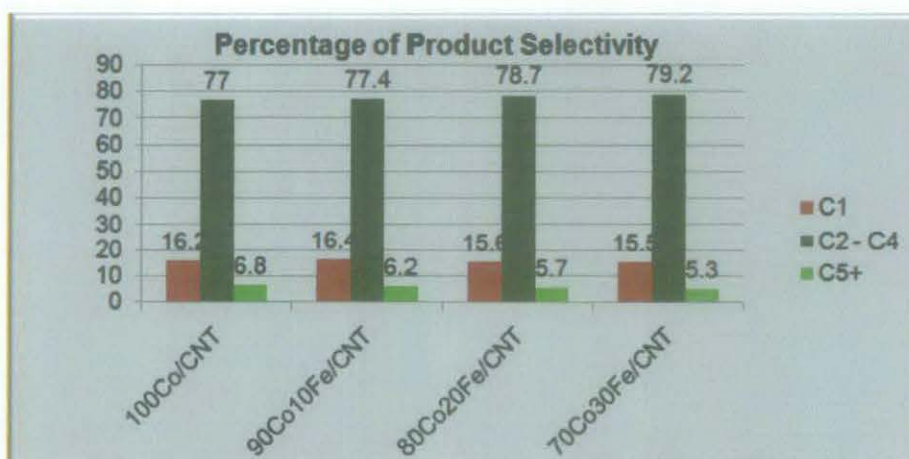


Figure 4.17: Percentage of product selectivity at different composition

From *Figure 4.17*, the product selectivity is increasing from 100Co/CNT to 70Co30Fe/CNT. The highest percentage of hydrocarbon selectivity is given by

70Co30Fe/CNT which is 79.2%. However, the selectivity of C₅₊ content is decreasing as the amount of Fe increase. In addition, selectivity of methane is also decreasing as the amount of Fe increases hence 70C030Fe/CNT has the lowest percentage in term of methane selectivity. As being discussed, in Fischer-Tropsch process, it is important to keep the catalyst at low methane selectivity and high amount of hydrocarbon product. From the bar chart, it can be concluded that 70Co30Fe/CNT has the most hydrocarbon and lowest methane production.

CHAPTER 5

CONCLUSION AND RECOMMENDATION

This project has been carried out using inert carbon nanotubes (CNT) as supporter for Co/Fe catalysts. The effects of different composition namely 100:0, 90:10, 80:20 and 70:30 have been experimented throughout the research. According to TEM result, average narrow particle size distributions approximately 5nm are found outside CNT 3nm are found inside of the supporter. The most distributed metal particle inside and outside the CNT base on the composition is 80Co20Fe/CNT base on the population standard deviation of the metals. The calculation from TEM analysis shows that 80Co20Fe/CNT nanocatalyst has the smallest population standard deviation which means it has the most uniform bimetallic distribution.

The result from FESEM is quite not significant, as it is hard to identify the distribution base only observing the electron images. BET provides more significant result as it gives the surface area value for each bimetallic nanocatalyst. The largest surface area among the nanocatalyst is 70Co30Fe/CNT which is $130.2439\text{m}^2/\text{g}$. Theoretically, a larger surface area can increase the reaction as more catalytic site are exposed to the reactant.

Base on Fischer-Tropsch performance of the microreactor, 90Co10Fe/CNT has the highest in term of CO conversion while 70Co30Fe/CNT has the highest product selectivity of 79.2%. C_1 and C_{5+} selectivity are reduced by 0.7% and 1.5% respectively. From this result, it can be concluded that 70Co30Fe/CNT is the most suitable nanocatalyst for Fischer-Tropsch process as it has the most uniform distribution and higher production of hydrocarbon as well as low selectivity of methane.

As being discussed, the size of particle does not really influence the performance of the catalyst. To further investigate the effect of the morphology and texture of the nanocatalyst, the nanocatalyst should be tested under appropriate temperature and pressure, equivalent to industrial operating condition.

As being studied, there are a lot of factors which can influence the performance of the catalyst. Thus, in future studies, other factors such as surfactant concentration, ratio of water to surfactant and the effect of pressure and temperature should be well studied to understand the catalysis process.

REFERENCES

- Abbaslou, R. M. M., Tavassoli, A., Soltan, J., & Dalai, A. K. (2009). Iron catalysts supported on carbon nanotubes for Fischer–Tropsch synthesis: Effect of catalytic site position. *Applied Catalysis A: General*, 367(1-2), 47-52.
- Capek, I. (1999). Radical polymerization of polar unsaturated monomers in direct microemulsion systems. *Advances in Colloid and Interface Science*, 80(2), 85-149.
- Dry, M., E. (1981). *The Fischer Tropsch Synthesis*, in: *Catalysis, Science and Technology*, eds, 1, 159-255.
- Duvenhage, D., J., & Coville, N., J. (1997). Fe:Co/TiO₂ bimetallic catalysts for the Fischer-Tropsch reaction 1. Characterization and reactor studies. *Applied Catalysis A: General*, 153, 43-67.
- Eriksson, S., Nylén, U., Rojas, S., & Boutonnet, M. (2004). Preparation of catalysts from microemulsions and their applications in heterogeneous catalysis. *Applied Catalysis A: General*, 265(2), 207-219.
- Haghshenas, M. (2010). Effects of Process Conditions on Production of Olefins from Synthesis Gas over a Cobalt Nanocatalyst. *World Applied Science Journal*, 10(2), 214-218.
- Iglesia, E. (1997). Design, synthesis and use of cobalt-based Fischer-Tropsch catalysts. *Applied Catalysis A: General*, 161, 59-78.
- Khodakov, A. Y., Chu, W., & Fongarland, P. (2007). Advance in the Development of Novel Cobalt Fischer-Tropsch Catalysts for Synthesis of Long-Chain Hydrocarbons and Clean Fuels. *Chem. Rev.*, 107, 1692-1744.
- Serp, P., Corrias, M., & Kalck, P. (2003). Carbon nanotubes and nanofibers in catalysis.

Applied Catalysis A: General, 253, 337-358.

Steynberg, A. P. (2004). Chapter 1 introduction to fischer-tropsch technology. In André Steynberg and Mark Dry (Ed.), *Studies in surface science and catalysis* (pp. 1-63) Elsevier.

Steynberg, A. P. (2004). Chapter 1 introduction to fischer-tropsch technology. In André Steynberg and Mark Dry (Ed.), *Studies in surface science and catalysis* (pp. 198) Elsevier.

Steynberg, A. P. (2004). Chapter 1 introduction to fischer-tropsch technology. In André Steynberg and Mark Dry (Ed.), *Studies in surface science and catalysis* (pp. 211) Elsevier.

Steynberg, A. P. (2004). Chapter 1 introduction to fischer-tropsch technology. In André Steynberg and Mark Dry (Ed.), *Studies in surface science and catalysis* (pp. 229) Elsevier.

Tavasoli, A., Trépanier, M., Malek Abbaslou, R. M., Dalai, A. K., & Abatzoglou, N. (2009). Fischer–Tropsch synthesis on mono- and bimetallic co and fe catalysts supported on carbon nanotubes. *Fuel Processing Technology*, 90(12), 1486-1494.

Trépanier, M., Dalai, A. K., & Abatzoglou, N. (2010). Synthesis of CNT-supported cobalt nanoparticle catalysts using a microemulsion technique: Role of nanoparticle size on reducibility, activity and selectivity in Fischer–Tropsch reactions. *Applied Catalysis A: General*, 374(1-2), 79-86.

Critical micelle concentration. (n.d.). Retrieved from <http://www.attension.com/critical-micelle-concentration.aspx>

Critical micelle concentration. (n.d.). Retrieved from <http://en.wikipedia.org>

[/wiki/Critical_micelle_concentration](#)

BET Surface Area & Gas Adsorption. (n.d.). Retrieved from http://www.quantachrome.co.uk/en/BET_Surface_Area_and_Gas_Adsorption.asp

Determination of the surface area by the BET method. (n.d.). Retrieved from http://zumbuhl lab.unibas.ch/pdf/talks/080425_Tobias_BET.pdf

Transmission Electron Microscopy (TEM) and Scanning Transmission Electron Microscopy (STEM). (n.d.). Retrieved from http://www.eaglabs.com/techniques/analytical_techniques/tem_stem.php

X-ray Diffraction. (n.d.). Retrieved from <http://www.panalytical.com/index.cfm?pid=135>

Background about X-Ray Diffraction. (n.d.). Retrieved from <http://www.geosci.ipfw.edu/xrd/techniqueinformation.html>

Catalysts characterization techniques. (n.d.). Retrieved from <http://herkules.oulu.fi/isbn9514269543/html/x900.html>

X-ray Photoelectron Spectroscopy. (n.d.). Retrieved from <http://www.phl.com/surface-analysis-techniques/xps.html>

X-ray Photoelectron Spectroscopy. (n.d.). Retrieved from <http://mee-inc.com/xray-photo.html>

LENNF EPSRC Facility – X-Ray Photoelectron Spectroscopy. (n.d.). Retrieved from <http://www.nanotechnology.leeds.ac.uk/lennf/facilities/SurfaceAnalysis.shtml>

X-ray Photoelectron Spectroscopy. (n.d.). Retrieved from <http://www-group.slac.stanford.edu/sms/xrayspectroscopy.html>

APPENDICES

APPENDIX CHAPTER 3

Appendix 3.1 Calculation of HNO₃ dilution

To dilute, an amount HNO₃, an amount of water is added into 65% volume of HNO₃ inside 250ml of volumetric flask as calculated below:

- CNT with 35% of HNO₃:

$$m_1v_1 = m_2v_2$$

$$65\% \times v_1 = 3\% \times 250\text{ml}$$

$$v_1 = 134.62\text{ml}$$

Hence, the appropriate amount of 65% HNO₃ inside 250ml of volumetric flask is 134.62ml.

Appendix 3.2 Calculation of metal precursor

The weight percent of metal to be introduced inside the supporter is 5 wt% whereas the mass loading for CNT for each sample is 0.475g. Thus, the appropriate amount of the metals is shown in the following table. The calculation for each sample is displayed as below:

Information:

- Mass loading of CNT: 0.475g
- Molecular weight of 5wt% Iron Nitrate, Fe(NO₃)₃.9H₂O: 404.00g/mol
- Molecular weight of 5wt% Cobalt Nitrate, Co(NO₃)₂.6H₂O: 291.04g/mol

➤ **Co:Fe (100:0)**

$$\text{Co: } (0.5\text{g} \times 5\text{wt\%})/100\% = 0.025\text{g}$$

$$\text{Hence, amount of cobalt nitrated needed: } (291.04\text{g/mol} \times 0.025\text{g})/59\text{g/mol} = 0.12\text{g}$$

➤ **Co:Fe (90:10)**

$$\text{Co: } (0.025\text{g} \times 90)/100 = 0.0225\text{g}$$

$$\text{Fe: } 0.025\text{g} - 0.0225\text{g} = 0.0025\text{g}$$

$$\text{Hence, amount of cobalt nitrate needed: } (291.04\text{g/mol} \times 0.0225\text{g})/59\text{g/mol} = 0.11\text{g}$$

$$\text{Amount of iron nitrate: } (404\text{g/mol} \times 0.0025\text{g})/56\text{g/mol} = 0.018\text{g/mol}$$

➤ **Co:Fe (80:20)**

$$\text{Co: } (0.025\text{g} \times 80)/100 = 0.02\text{g}$$

$$\text{Fe: } 0.025\text{g} - 0.02\text{g} = 0.005\text{g}$$

$$\text{Hence, amount of cobalt nitrate needed: } (291.04\text{g/mol} \times 0.02\text{g})/59\text{g/mol} = 0.098\text{g}$$

$$\text{Amount of iron nitrate needed: } (404\text{g/mol} \times 0.005\text{g})/56\text{g/mol} = 0.0367\text{g}$$

➤ **Co:Fe (70:30)**

$$\text{Co: } (0.025\text{g} \times 70)/100 = 0.0175\text{g}$$

$$\text{Fe: } 0.025\text{g} - 0.0175\text{g} = 0.0075\text{g}$$

$$\text{Hence, amount of cobalt nitrate needed: } (291.04 \times 0.0175\text{g})/59\text{g/mol} = 0.086\text{g}$$

$$\text{Amount of iron nitrate needed: } (404\text{g/mol} \times 0.0075\text{g})/56\text{g/mol} = 0.0541\text{g}$$

Appendix 3.3 Calculation of surfactant and cyclohexane

The volume of cyclohexane needed to dilute n mol of Triton X-114 is shown as follows:

$$0.2 \text{molar}_{\text{Triton}} = n_{\text{Triton}} / v_{\text{cyclohexane}}$$

$$n_{\text{Triton}} = 0.1 \text{litre}_{\text{cyclohexane}} \times 0.2 \text{molar}_{\text{Triton}}$$

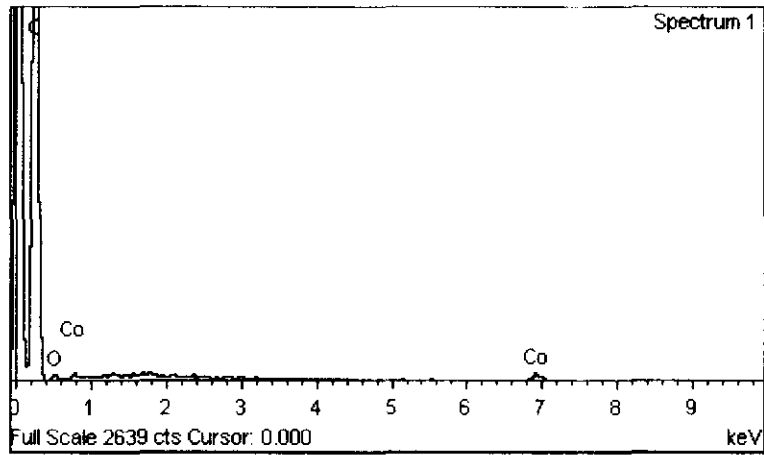
$$n_{\text{Triton}} = 0.02 \text{mol}_{\text{Triton}}$$

$$\text{Mass}_{\text{Triton}} = 0.02 \text{mol} \times \text{Molar Mass}_{\text{Triton}} = 0.02 \text{mol} \times 558.75 \text{g/mol} = 11.175 \text{g}_{\text{Triton}}$$

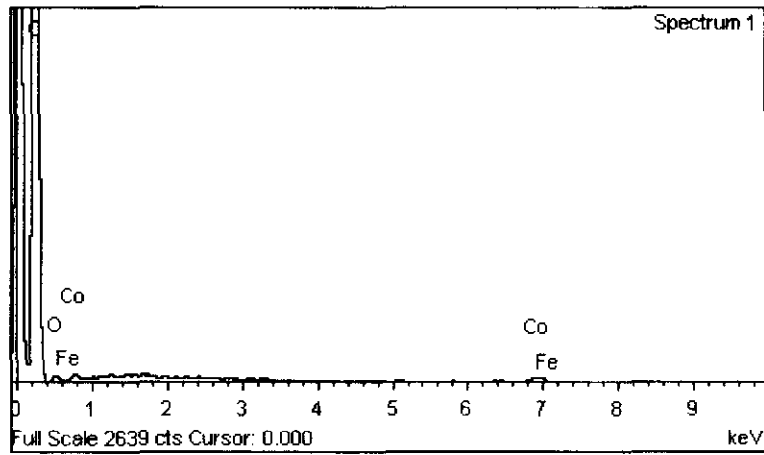
*Note that the molecular weight of Triton X-114 is 558.75g/mol.

APPENDIX CHAPTER 4

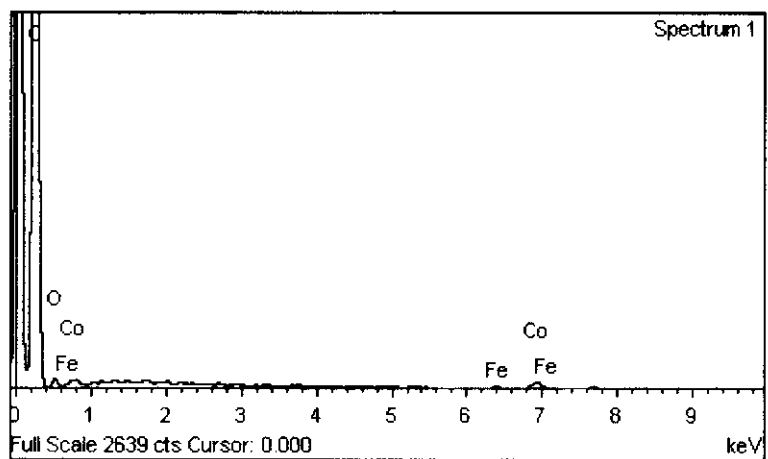
Appendix 4.1 Spectrum processing from FESEM



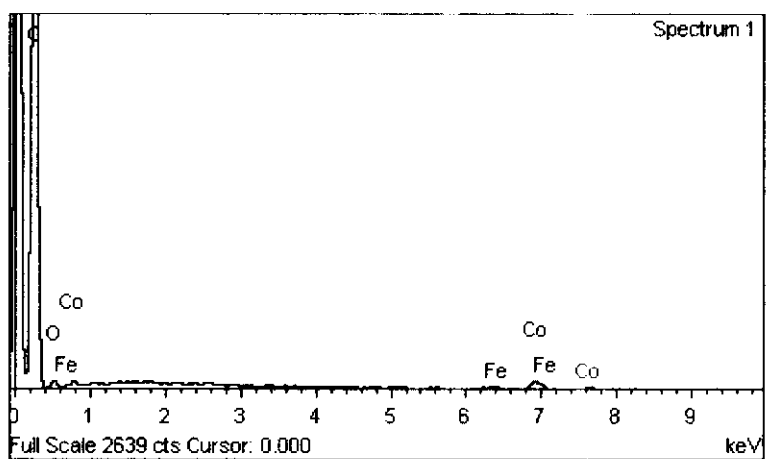
Spectrum processing on 100Co/CNT nanocatalyst



Spectrum processing on 90Co10Fe/CNT nanocatalyst

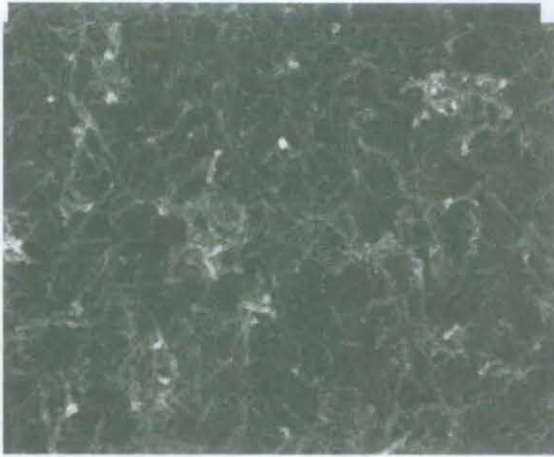


Spectrum processing on 80Co20Fe/CNT nanocatalyst

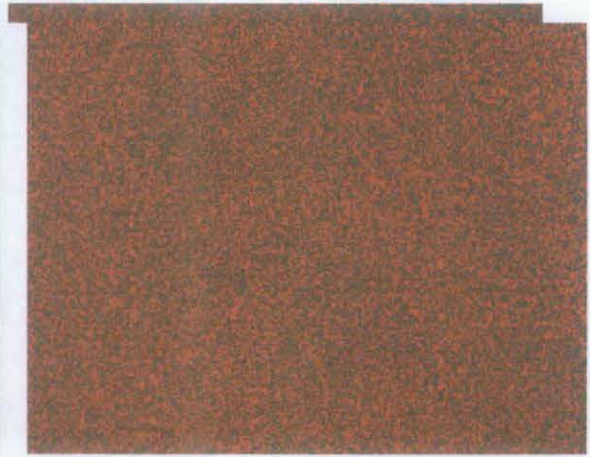


Spectrum processing on 70Co30Fe/CNT nanocatalyst

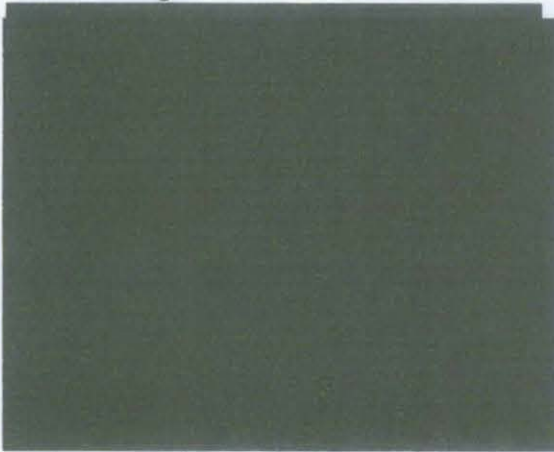
Appendix 4.2 Electron images from EDX



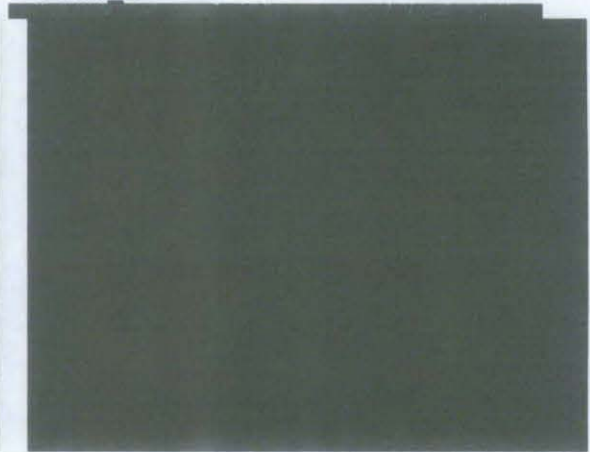
Electron Image 1



C Ka1_2



Co Ka1



Fe Ka1

EDX images of CNT, Co and Fe distribution for 100Co/CNT



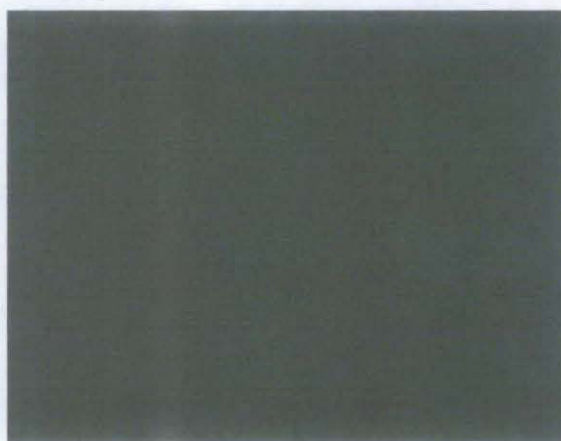
Electron Image 1



C Ka1_2



Co Ka1

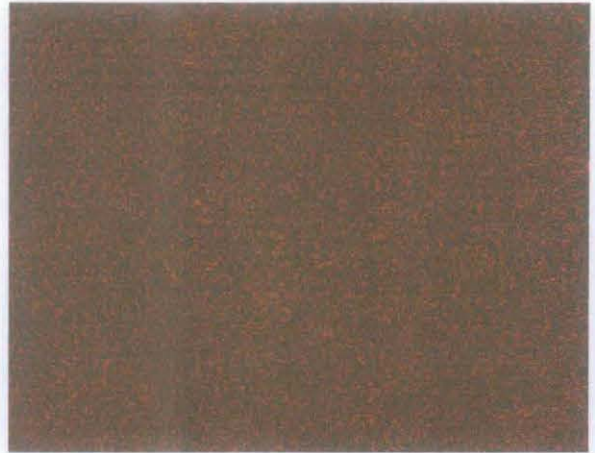


Fe Ka1

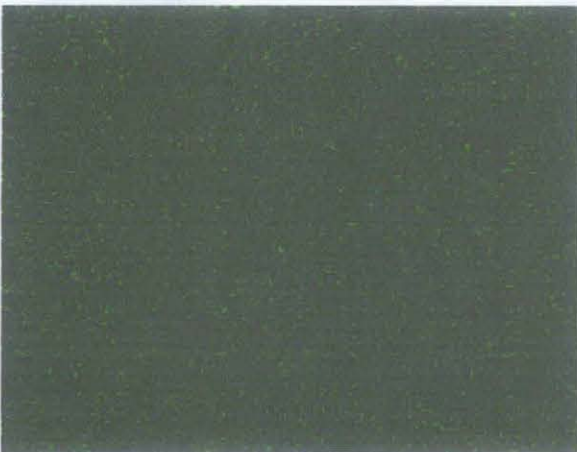
EDX images of CNT, Co and Fe distribution for 90Co10Fe/CNT



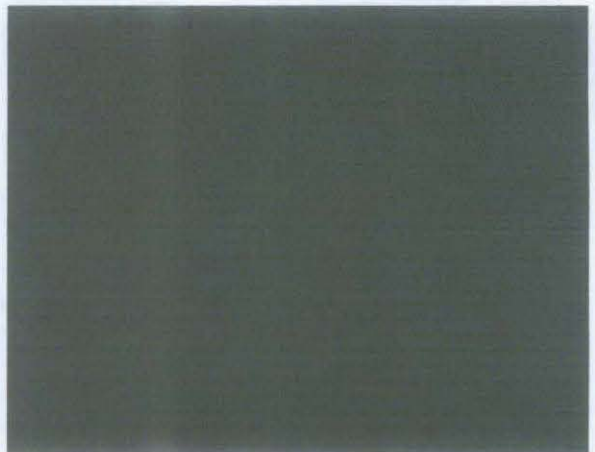
Electron Image 1



C Ka1_2



Co Ka1

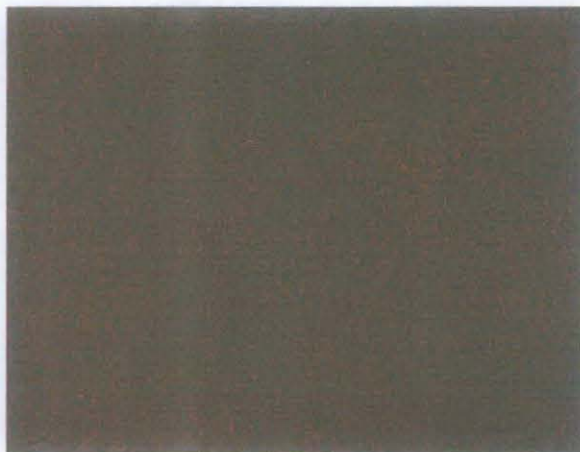


Fe Ka1

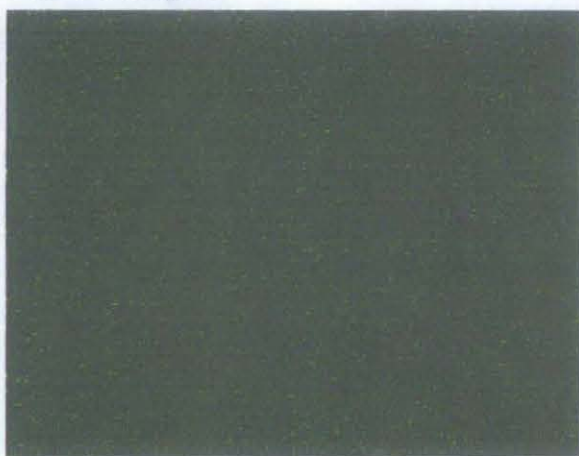
EDX images of CNT, Co and Fe distribution for 80Co20Fe/CNT



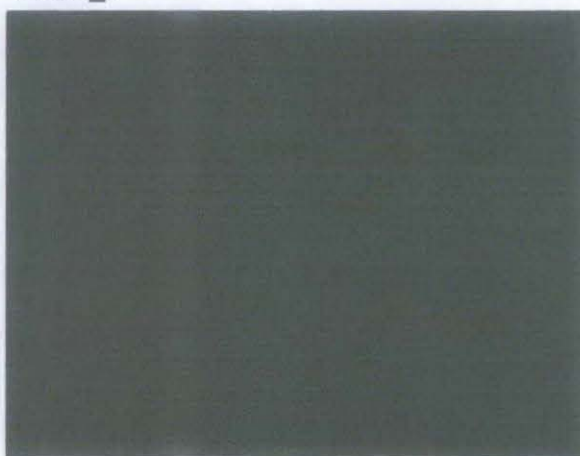
Electron Image 1



C Ka1_2



Co Ka1



Fe Ka1

EDX images of CNT, Co and Fe distribution for 70Co30Fe/CNT

Appendix 4.3 Calculation of average particle size and population standard deviation

No.	Size	100Co	90Co10Fe	80Co20Fe	70Co30Fe	M1	M2	M3	M4
1	0.962	0	0	0	0	0	0	0	0
2	1.924	1	1	2	1	1.924	1.924	3.848	1.924
3	2.886	15	19	10	13	43.29	54.834	28.86	37.518
4	3.848	28	36	42	34	107.744	138.528	161.616	130.832
5	4.81	26	37	55	42	125.06	177.97	264.55	202.02
6	5.772	12	10	22	19	69.264	57.72	126.984	109.668
7	6.734	8	11	11	19	53.872	74.074	74.074	127.946
8	7.696	2	10	3	5	15.392	76.96	23.088	38.48
9	8.658	0	3	3	5	0	25.974	25.974	43.29
10	9.62	0	4	4	1	0	38.48	38.48	9.62
11	10.582	0	2	0	2	0	21.164	0	21.164
12	11.544	0	0	0	1	0	0	0	11.544
13	12.506	0	0	1	0	0	0	12.506	0
14	13.468	0	0	0	0	0	0	0	0
15	14.43	0	0	0	0	0	0	0	0
16	15.392	0	0	1	0	0	0	15.392	0
17	16.354	0	0	0	0	0	0	0	0
18	17.316	0	0	0	0	0	0	0	0
19	18.278	0	1	0	0	0	18.278	0	0
20	19.24	0	0	0	0	0	0	0	0
Total		92	134	154	142	416.546	685.906	775.372	734.006

Average Particle Size (M)			
S1	S2	S3	S4
4.527674	5.118701	5.034883	5.169056

(X-M)^2			
S1	S2	S3	S4
12.71403	17.27817	16.58838	17.69932
3.701776	3.701776	3.701776	3.701776
8.328996	8.328996	8.328996	8.328996
14.8071	14.8071	14.8071	14.8071
23.1361	23.1361	23.1361	23.1361
33.31598	33.31598	33.31598	33.31598
45.34676	45.34676	45.34676	45.34676
59.22842	59.22842	59.22842	59.22842
74.96096	74.96096	74.96096	74.96096
92.5444	92.5444	92.5444	92.5444
111.9787	111.9787	111.9787	111.9787
133.2639	133.2639	133.2639	133.2639
156.4	156.4	156.4	156.4
181.387	181.387	181.387	181.387
208.2249	208.2249	208.2249	208.2249
236.9137	236.9137	236.9137	236.9137
267.4533	267.4533	267.4533	267.4533
299.8439	299.8439	299.8439	299.8439
334.0853	334.0853	334.0853	334.0853
370.1776	370.1776	370.1776	370.1776
Total	2667.813	2672.377	2671.687

Standard Deviation			
S1	S2	S3	S4
28.99797	19.94311	17.34862	18.82252
5.385	4.466	4.165	4.338